



HAL
open science

From fruit growth to ripening in plantain: a careful balance between carbohydrate synthesis and breakdown

N.A. Campos, Sophie Colombie, Annick Moing, Cédric Cassan, D. Amah, R. Swennen, Yves Gibon, S.C. Carpentier, Sebastien Carpentier

► To cite this version:

N.A. Campos, Sophie Colombie, Annick Moing, Cédric Cassan, D. Amah, et al.. From fruit growth to ripening in plantain: a careful balance between carbohydrate synthesis and breakdown. 2021. hal-03659204

HAL Id: hal-03659204

<https://hal.inrae.fr/hal-03659204v1>

Preprint submitted on 4 May 2022

HAL is a multi-disciplinary open access archive for the deposit and dissemination of scientific research documents, whether they are published or not. The documents may come from teaching and research institutions in France or abroad, or from public or private research centers.

L'archive ouverte pluridisciplinaire **HAL**, est destinée au dépôt et à la diffusion de documents scientifiques de niveau recherche, publiés ou non, émanant des établissements d'enseignement et de recherche français ou étrangers, des laboratoires publics ou privés.



Distributed under a Creative Commons Attribution - NonCommercial - NoDerivatives 4.0 International License

32

33 **Abstract**

34 We investigated the fruit development in two plantain banana cultivars from two weeks
35 after bunch emergence till twelve weeks through high-throughput proteomics, major metabolite
36 quantification and metabolic flux analyses. We give for the first time an insight at early stages of
37 starch synthesis and breakdown. Starch and sugar synthesis and breakdown are processes that
38 take place simultaneously. During the first eight to ten weeks the balance between synthesis and
39 breakdown is clearly in favour of sugar breakdown and a net starch synthesis occurs. During this
40 period, plantain fruit accumulates up to 48% of starch. The initiation of the ripening process is
41 accompanied with a shift in balance towards net starch breakdown. The key enzymes related to
42 this are phosphoglucan water dikinase (PWD), phosphoglucan phosphatase, α -1,6-glucosidase
43 starch debranching enzyme (DBE), alpha glucan phosphorylase (PHS) and 4-alpha
44 glucanotransferase disproportioning enzyme (DPE). The highest correlations with sucrose have
45 been observed for PHS and DPE. There is also a significant correlation between the enzymes
46 involved in ethylene biosynthesis, starch breakdown, pulp softening and ascorbate biosynthesis.
47 The faster ending of maturation and starting of ripening in the Agbagba cultivar are linked to the
48 key enzymes 1-aminocyclopropane-1-carboxylate oxidase and DPE. This knowledge of the
49 mechanisms that regulate starch and sugar metabolisms during maturation and ripening is
50 fundamental to determine the harvest moment, reduce postharvest losses and improve final
51 product quality of breeding programs.

52

53 **1 Introduction**

54

55 Fruit development is a complex phenomenon that encompasses several overlapping
56 stages: cell division, cell enlargement, maturation, ripening and senescence (Paul et al., 2012). At
57 the initiation of fruit development, fruits enlarge mainly through cell division and they reach
58 their final size by increasing cell volume. The active cell division and cell expansion are
59 accompanied by a net accumulation of storage products until full maturation. Ripening induces
60 changes in flavour, texture, colour, and aroma. Fruits can be divided into two groups with
61 contrasting ripening mechanisms. Climacteric fruit (such as tomato, avocado, apple, and banana)
62 are linked to ethylene biosynthesis and an increase in respiration which induces ripening (White,
63 2002). During maturation, two systems of ethylene are operational: system 1 and system 2.
64 During early maturation, system 1 is active and the rate of ethylene production is basal and there
65 is an auto-inhibition of ethylene production. But as maturation progresses, this inhibition process
66 is stopped and there is an auto-induction of ethylene production leading to the onset of ripening
67 (Paul et al., 2012).

68 Edible bananas are parthenocarpic and so the ovaries develop into seedless fruits without
69 pollination stimulus. The pulp-initiating cells are situated within the inner epidermis of the fruit
70 pericarp and septa. In parthenocarpic bananas, those cells start to proliferate very fast after
71 flowering (bunch emergence) (Ram et al., 1962). The increase in cell number in the initiating
72 region of the pulp continues up to about 4 Weeks After bunch Emergence (WAE). Then it
73 subsides and growth is largely realized by cell enlargement (Ram et al., 1962). Sugar deposition
74 and starch synthesis in the pulp cells commence very early and they become well established by
75 8 WAE. The first signs of starch disappearance have been reported to be around 12 WAE (Ram
76 et al., 1962). However, this is dependent on the environment and on the genotype. Depending on
77 the genotype, banana fruit has been reported to accumulate between 12 and 35% of starch during
78 4-8 WAE and from 8 WAE starch content drops to between 15 and 0% in late stages of
79 maturation (Soares et al., 2011; Cordenunsi-Lysenko et al., 2019). Plantains are part of the group
80 of bananas that accumulate a large amount of starch. At ripe stage, plantains still have a high
81 starch content, which affects their taste (Soares et al., 2011). Therefore, plantains are not suitable
82 as sweet dessert bananas and are consumed as starch source. The current practice is to harvest
83 when fruits of the first hand show signs of ripening (Dadzie and Orchard, 1997). Plantains are an

84 important staple food in tropical and subtropical countries, being of special importance in West-
85 Africa (Vuylsteke et al., 1993). Genetically, they are triploids and belong to the AAB genotype
86 group. They are a product of a natural cross between *Musa acuminata* (A genotype) and *Musa*
87 *balbisiana* (B genotype) (Simmonds, 1962). And although morphologically they are quite
88 diverse, genetically they are extremely uniform (Crouch et al., 2000). The recent release of the B
89 genome suggested a dominance of genes related to starch metabolism, leading to a higher starch
90 accumulation during fruit development (Wang et al., 2019). A better understanding of the
91 mechanisms that regulate sugar primary metabolism during fruit development will be important
92 to select hybrids with the best post-harvest traits.

93 Most papers are focused on Cavendish sweet banana that is the most exported banana
94 cultivar in the world (Agopian et al., 2008; Toledo et al., 2012; Asif et al., 2014; Du et al., 2016).
95 Recently, we published the first proteome of plantain fruit and a comparison of the proteomes of
96 Cavendish and plantain during the final ripening process (Campos et al., 2018; Bhuiyan et al.,
97 2020). Together with the recent update from the B genome sequence (Wang et al., 2019), these
98 works are contributing to elucidate the fruit development in plantain as well to determine the role
99 of the B genome in fruit quality. In complement to proteome studies, metabolic flux can be
100 predicted using constraint-based models based on metabolic network description through
101 stoichiometric equations of reactions, and on the assumption of pseudo-steady state and the
102 choice of an objective function (Orth et al., 2010). Such knowledge-based stoichiometric models
103 describing central metabolism have already proved useful in tomato fruit to estimate fluxes
104 throughout the development and to show that carbon degraded from starch and cell wall
105 generated an excess of energy dissipated just before the onset of ripening coinciding with the
106 respiration climacteric (Colombié et al., 2015; Colombié et al., 2017). By combining proteomics
107 and flux studies, we gain here unique insights into the order of appearance and dominance of
108 specific enzymes/fluxes involved in starch synthesis and breakdown and sugar synthesis in
109 plantain fruit.

110

111 **2 Material and Methods**

112

113 *2.1 Biological Material*

114 The biological samples were collected from the IITA Experimental Field in Ibadan,
115 Nigeria, during the period from October 2016 to February 2017.

116 Five banana plants from Agbagba and Obino L'Ewai cultivars were selected and the
117 same plants were followed during all the experiment. One fruit per plant was collected from 2
118 WAE until the fruits reached full maturity. The collected fruits were cleaned and measurements
119 of fruit length (L) and circumference (C) were taken. For the fruit volume calculation our
120 formula was based on (Simmonds, 1953). To know the correlation between fruit weight,
121 calculated fruit volume and real fruit volume, the real volume of representative fruits was
122 measured by submerging the them in water in a measuring cylinder. For the remainder of the
123 fruits, the volume was calculated with the formula: $\text{Volume (cm}^3\text{)} = ((\text{Fruit length} * (\text{Fruit}$
124 $\text{circumference})^2 * 0.0616) + 0.3537)$. After determination of fruit length and circumference, the
125 fruit was separated from the peels, cut in smaller pieces and stored at $- 80\text{ }^\circ\text{C}$ until
126 lyophilization. Samples were lyophilized to ensure a safe transportation from Nigeria to Belgium
127 and to facilitate the protein and metabolite extraction process (Carpentier et al., 2007). The
128 lyophilized samples were then, sent to Belgium where the protein extraction, quantification and
129 identification were performed and to France for metabolite analysis.

130

131 *2.2 Protein extraction, quantification, identification and annotation*

132 Extractions were performed following the phenol-extraction/ammonium-acetate
133 precipitation protocol described previously (Carpentier et al., 2005; Buts et al., 2014). Samples
134 of 2 and 4 WAE could not be analyzed through proteomics due to the presence of many
135 interfering compounds disturbing the correct application of the protocol.

136 After extraction, 20 μg of proteins were digested with trypsin (Trypsin Protease, MS
137 Grade ThermoScientific, Merelbeke, Belgium) and purified by Pierce C18 Spin Columns
138 (ThermoScientific, Merelbeke, Belgium). The digested samples (0.5 $\mu\text{g}/5\mu\text{L}$) were separated in
139 an Ultimate 3000 (ThermoScientific) UPLC system and then in a Q Exactive Orbitrap mass
140 spectrometer (ThermoScientific) as described (van Wesemael et al., 2018). For protein
141 quantification, we used the software Progenesis® (Nonlinear Dynamics). In this software we

142 used MASCOT version 2.2.06 (Matrix Science) against the Musa V2 database of *M. acuminata*
143 and *M. balbisiana* (Martin et al., 2016; Wang et al., 2019) (157832 proteins). Tandem mass
144 spectra were extracted by Progenesis. All MS/MS spectra were searched with a fragment ion mass
145 tolerance of 0,02 Da and a parent ion tolerance of 10 PPM. Carbamidomethyl of cysteine was
146 specified in Mascot as a fixed modification. Deamidation of asparagine and glutamine and
147 oxidation of methionine were specified in Mascot as variable modifications and the results were
148 reintroduced in Progenesis. Scaffold (version Scaffold_4.11.0, Proteome Software) was used to
149 validate MS/MS based peptide and protein identifications. Peptide identifications were accepted
150 if they could be established at greater than 95,0% probability by the Peptide Prophet algorithm
151 with Scaffold delta-mass correction (Keller et al., 2002; Searle, 2010). Protein identifications
152 were accepted if they contained at least 1 identified peptide. Protein probabilities were assigned
153 by the Protein Prophet algorithm (Nesvizhskii et al., 2003). Proteins that contained similar
154 peptides and could not be differentiated based on MS/MS analysis alone were grouped to satisfy
155 the principles of parsimony. Proteins sharing significant peptide evidence were grouped into
156 clusters. A protein false discovery rate of 0.8% and a spectral false discovery rate of 0.04% was
157 observed by searching the reverse concatenated decoy database (157832 proteins). All data have
158 been made available in the public repository PRIDE under the project name: Carbohydrate
159 metabolism during plantain development, Project accession: PXD029901 and Project DOI:
160 10.6019/PXD029901.

161 Gene annotations were taken from the banana Hub (Droc et al., 2013) and verified in Plant
162 Metabolic Network (Hawkins et al., 2021) and Prosite (Expasy SIB Bioinformatics Resource
163 Portal). Subcellular prediction were analyzed via the software DeepLoc 1.0 (Almagro
164 Armenteros et al., 2017).

165

166 2.3 Metabolic Analysis

167 To complement our proteomics data and improve our insights about plantain fruit
168 development, we analyzed major metabolic traits in pulp. Metabolites were extracted from 10
169 mg aliquots of lyophilized ground samples via three successive extractions with ethanol-buffer
170 mixtures successively composed of 80, 80 and 50% ethanol and 10 mM HEPES/KOH buffer (pH
171 6). The supernatants were collected and pooled in order to measure soluble metabolites. Glucose,
172 fructose and sucrose were measured enzymatically (Stitt et al., 1989). Glucose-6-phosphate,

173 fructose-6-phosphate and glucose-1-phosphate were measured using an enzyme cycling assay
174 (Gibon et al., 2002). Malate was measured enzymatically as in (Mollering, 1985). Total free
175 amino acids were measured using fluorescamine (Bantan-Polak et al., 2001). Polyphenols were
176 measured using Folin-Ciocalteu's reagent (Blainski et al., 2013). In order to quantify the total
177 protein content, the pellets were resuspended in 100 mM NaOH and then heated for 20 min.
178 After centrifugation (5,000 g, 5 min), the total protein content was measured with Coomassie
179 Blue (Bradford, 1976). After neutralization with HCl, starch was quantified in the pellets as
180 described previously (Hendriks et al., 2003). Finally, the pellet was washed twice with water and
181 twice with ethanol 96% v/v, dried and weighed to estimate the cell wall content.

182

183 *2.4 Flux calculation by constrain-based modelling*

184 A flux-balance model was constructed by integrating biochemical and physiological knowledge
185 about central metabolism previously described (Colombié et al., 2015; Soubeyrand et al., 2018)
186 dedicated to breakdown and transformation of extracellular nutrients to produce energy and
187 metabolites and a specialized metabolic pathway producing the main polyphenol compounds.
188 Energy intermediates, both ATP and NAD(P)H, were explicitly considered and all the cofactors
189 were defined as internal metabolites, which means that they were balanced, thus constraining the
190 metabolic network not only through the carbon and nitrogen balance but also through the redox
191 and energy status.

192 To solve the flux balance model, constraints were applied for (1) flux reversibility or
193 irreversibility and for (2) outfluxes boundaries. Therefore, concentrations of accumulated
194 metabolites and biomass components, expressed on a mole per fruit basis, were fitted to calculate
195 the corresponding fluxes. Stoichiometric network reconstruction encompassing central and
196 polyphenol metabolism and mathematical problems were implemented using MATLAB
197 (Mathworks R2012b, Natick, MA, USA) and the optimization toolbox, solver quadprod with
198 interior-point-convex algorithm for the minimization. Flux maps were drawn with the flux
199 visualization tool of VANTED 2.1.0.

200

201 *2.5 Statistical analyses*

202 For proteins, statistical analyses were made using the software Statistica 8 (TIBCO)
203 based on the exported protein quantifications of Progenesis. We performed a principal

204 component analysis (PCA, with NIPALS algorithm) to get an overview of the proteome data. We
205 performed a partial least squares analysis (PLS) (NIPALS algorithm) to differentiate proteins
206 with a significant correlation to the time points, the genotype, metabolite using all protein
207 quantifications as continuous predictors (x matrix) and the time points, genotype and quantified
208 metabolite as dependent variables (y matrix). We applied a two-way ANOVA ($P<0.05$) to the
209 selected proteins to verify their significance affected by the time point, genotype or the
210 interaction between both.

211 For metabolites, a principal component analysis was performed on the averages per
212 cultivar and time point.

213 All displayed regressions were made in Microsoft excel and based on the best fit R^2 . Pearson
214 correlations between proteins or between proteins and selected metabolites or other variables
215 were calculated with Statistica 8 (TIBCO).

216 To integrate the different omics data, the protein inference and isoform redundancy issue was
217 tackled by quantifying the proteins at protein cluster level and EMPAI quantification
218 (Scaffold_4.11.0, Proteome Software). To find the protein clusters that correlated to the
219 modelled fluxes, we performed a two-block sparse partial-least-squares discriminant analysis
220 (sPLS-DA) with mixOmics package of R (Rohart et al., 2017) using DIABLO application (Singh
221 et al., 2019) with default parameters. To the relationships between the proteins and fluxes were
222 calculated with $P<0.001$ (after false discovery rate [FDR] correction) threshold for Pearson
223 correlations.

224

225 **3 Results**

226 *3.1 The different growth stages are characterized by a particular proteome and metabolic profile*

227 Based on an unsupervised principal component analysis, the proteome differed at each time point
228 (Figure 1). The first component explained 23% of total variability and clearly separated the
229 different time points. The second component explained 17% of total variability, and was
230 correlated to the cultivar. Both cultivars had a similar proteome except for the last time point at
231 12 Weeks After bunch Emergence (WAE). The same is true for the metabolite and the flux
232 analysis data, expect that the largest difference between the two cultivars is observed at 6 WAE
233 for the metabolites and both at 6 and 12 WAE for the fluxes (Figure S1).

234

235 Concerning fruit growth, in both cultivars we observed a sigmoid curve with three growth
236 phases: a fast growth phase (0-6 WAE), a phase of slow growth (6-8 WAE) and a second phase
237 of fast growth (8-12 WAE) (Figure 2, S2). Based on the observed abundance pattern of Sucrose
238 Synthase (SuSy) and invertase, we hypothesize that the first fast growth phase is completely
239 dominated by Sucrose Synthase (SuSy), while the third growth phase is dominated by invertase.
240 The abundance of invertase showed an excellent correlation with the growth rate (Figure 3).

241
242 We did find evidence to confirm the involvement of cell division in growth in our proteomics
243 data. Based on the identified histone proteins we deduce that cell division takes place up till 8
244 WAE (Table 1). A fast cell division is also accompanied with a high activity of cell wall building
245 and modifying enzymes (UDP-glucose 6-dehydrogenase, UDP-glucuronic acid decarboxylase,
246 Beta-glucosidase), mRNA translation (eukaryotic initiation factors, ribosomal proteins), protein
247 folding (T-complex proteins) and turnover (proteasome complex) (Table 1). The identified
248 proteins involved in the cell division processes significantly decrease in abundance from 6
249 WAE.
250 *3.2 Starch and sugar metabolism: synthesis and breakdown are processes that take place simultaneously*

251 The pulp at 6 WAE contained three times more fructose than glucose, but the concentration of
252 fructose represented <1 % of that of starch and less than 15% of that of sucrose. Among the
253 hexose phosphates, the amount of Glc-6-P was 20-fold higher than Glc-1-P (Table 2). The pulp at
254 12 WAE contained twice more fructose than glucose, but the concentration of fructose
255 represented <0.5 % of that of starch and less than 5% of that of sucrose. Among the hexose
256 phosphates, the amount of Glc-6-P was 20-fold higher than Glc-1-P (Table 2).

257
258 The accumulation of starch in the pulp cells started very fast and was the highest between 0 and
259 2 WAE (Figure 4). The balance between the synthesis and the breakdown was clearly in favour
260 of starch synthesis breakdown during the first 8-10 WAE resulting in a net increase in starch
261 content (Figure 4). During the net starch accumulation period, plantain fruit accumulated up to
262 48% (DW) of starch (Table 2).

263
264 *3.2.1 Starch synthesis*
265

266 Next to the high abundance of fructose and glucose-6-phosphate (Table 2), a high abundance of a
267 glucose-6-phosphate translocator (6), phosphoglucomutase (5) the glucose-1-phosphate
268 adenyltransferase (2) and plastidic fructokinase (12) was observed (Table 3, Figure 6A). We
269 did identify a so far uncharacterized sugar translocator (11) (Ma10_p26490) that has an almost
270 perfect correlation ($p < 0.0001$, $R = 0.99$) with SuSy (1) (Table 3, Figure 5).).

271
272 Following the uptake of glucose-6-P into the pulp amyloplast, starch synthesis starts via the
273 concerted action of phosphoglucomutase (7), glucose-1-phosphate adenyltransferases
274 (AGPase) (8) and the starch polymerizing reactions (9, 10) (Table 3, Figure 6A). In case of
275 fructose, the action of fructokinase (12) and glucose-6-phosphate isomerase (13) are required
276 (Table 3, Figure 6A). The soluble starch synthase (10) decreased in abundance during the further
277 development while granule bound starch synthase raised in abundance (9) (Table 3).
278 Amyloplasts have to import ATP coming from respiration via the cytosol through an ATP/ADP
279 transport protein (19). This enzyme is highly abundant when starch synthesis is high (Table 3,
280 Figure 6A).

281 Beyond their role as intermediates in the conversion of sucrose to starch, hexose phosphates also
282 serve as substrates for glycolysis and the oxidative pentose phosphate pathway. The significant
283 correlation to starch from pyrophosphate-fructose 6-phosphate 1-phosphotransferase (15) and
284 glyceraldehyde-3-phosphate dehydrogenase (18) (Table 3) is probably due to their function in
285 the glycolysis. Whereas in chloroplasts the ATP necessary for starch synthesis is provided
286 through photosynthesis, in pulp the amyloplasts have to import ATP coming from respiration via
287 the cytosol through an ATP/ADP transport protein (19). This enzyme is highly abundant when
288 starch synthesis is high (Table 3, Figure 6A).

289

290 *3.2.2 Starch breakdown*

291

292 The enzymes phosphoglucan water dikinase (PWD) (21), phosphorylase (20), phosphoglucan
293 phosphatases (22), α -1,6-glucosidase starch debranching enzyme (DBE) (23) and 4- α -
294 glucanotransferase disproportionating enzymes (DPE) (24) and the transporters glucose-6P
295 transporter (6) and the plastidic glucose transporter (25) increased significantly in abundance
296 over time (Table 3, Figure 6B).

297

298 *3.3 Sucrose synthesis*

299 The concentration of sucrose significantly increases with time (Table 2). The enzymes with the
300 highest correlation to sucrose were 4- α -glucanotransferase Disproportionating enzymes (DPE)
301 (24), Alpha-1,4 glucan phosphorylase (20) and Phosphoglucomutase, chloroplastic (7) (Table 3).
302 UTP-glucose-1-phosphate uridylyltransferase (2) was one of the most abundant proteins in pulp
303 and its abundance increased with time (Table 3, Figure 6). The production of UGP-glucose can
304 lead to sucrose synthesis either through SuSy (1), which is still abundantly present, or through
305 sucrose-phosphate synthase (27) which had its highest abundance at 12 WAE (Table 3, Figure
306 6B).

307 The formed sucrose can then be transported to the vacuole for storage or further processing or
308 can be degraded by invertase (29) and/or SuSy (1) (Table 3, Figure 6B). Invertase (29)
309 Mba10_g13890.1, is only encoded on the B genome and is predicted via the software DeepLoc
310 1.0 (Almagro Armenteros et al., 2017) to be localized in the cytoplasm. The cytoplasmatic
311 homologue coded on the acuminata genome is most probably not or expressed in a very low
312 level since we did not find a confident specific spectrum. Part of the metabolized sucrose is most
313 likely also transported to the vacuole since we have identified a monosaccharide transporter (30)
314 (Ma04_p22640.1;Mba04_g23280.1) that has the highest abundance at 12 WAE (Table 3, Figure
315 6B). DeepLoc predicts the membrane protein to the plasma membrane with a likelihood of 0.49
316 and to the vacuole with a likelihood of 0.35. Since no cell wall invertase has been identified and
317 since we did identify invertase in the cytoplasm, we assume that the monosaccharide transporter
318 (30) is located in the vacuolar membrane (Figure 6B). Also the upregulation of the vacuolar
319 pyrophosphate energized proton pump (28) (Ma07_p22370.1) (Table 3) facilitates the transport
320 of sugars across the vacuolar membrane. We have observed an increased abundance of soluble
321 inorganic pyrophosphatase, in the amyloplast (26) and at the vacuole (28) that coincides with the
322 decrease in starch synthesis and increase in sugars. (Tables 2, 3, Figure 6B).

323

324 *3.4 Cultivar specific ripening*

325 Proteins involved in ascorbate synthesis (GDP-mannose 3,5-epimerase) and anti-oxidant defense
326 (ascorbate peroxidase, Monodehydroascorbate reductase) had their highest abundance at 12
327 WAE (Table 4). The increase in sucrose production in time is significantly correlated to 1-

328 aminocyclopropane-1-carboxylate oxidase (ACO) (Table 4). We see a cultivar specific
329 interaction between cultivar and WAE meaning that the abundance of ACO changes differently
330 over time in both cultivars (Table 4). A pectinesterase related protein and a lichenase were
331 correlated to both sugar and ACO (Table 4). We did find a GLP (Germin-like protein 12-1)
332 protein that has a significant correlation with ACO (Table 4). A prosite scan shows that the
333 protein has a Fe(2+) 2-oxoglutarate dioxygenase domain profile. The protein had moreover also a
334 cultivar specific pattern associated to the earlier ripening Agbagba cultivar (Table 4). We
335 observed an excellent correlation between ACO and a sorbitol dehydrogenase, which catabolize
336 sorbitol into fructose (Fru) and glucose (Glu). Also here the cultivar Agbagba had a significantly
337 earlier response than Obino '1 Ewai (Table 4).
338 *3.5 The global flux decreased throughout fruit development*

339 The measured concentrations of the biomass and the accumulated metabolites in the pulp,
340 determined at 2, 4, 6, 8, 10 and 12 WAE (Table 2) were fitted to calculate the corresponding
341 fluxes used as constraints in the metabolic model. The estimated fluxes showed the highest
342 activity for fluxes involved in respiration, glycolysis and TCA cycle (Figure S3). At the early
343 stage of development (Figure 7, 2 WAE) those fluxes had their highest activity and a global
344 decrease throughout fruit development was noticed, in agreement with metabolic fluxes
345 described on tomato fruit (Colombié et al., 2015). This decrease in flux activity throughout fruit
346 development was similar in both cultivars. We assessed that a high respiration is associated with
347 the cell division associated with the first growth phase followed by a global decrease in flux
348 activity during the second and third-growth phase, where only elongation takes place. No
349 increase in respiration was detected at the end of the maturation, probably because the burst did
350 not take place yet in the investigated fruits.

351
352 The flux analysis complemented the proteome data (Figures 6 A and B). Nice concordance was
353 observed for major reactions in starch biosynthesis: sucrose synthase (1), fructokinase (3),
354 glucose-6-phosphate isomerase (4), and glucose-1-phosphate adenylyltransferase (8) (Figure
355 6A).

356 For the flux at 12 WAE in the starch degradation pathway (Figure 6B) next to invertase (29) also
357 fluxes through sucrose synthase (1), and glucose-6-phosphate isomerase (4) pointed towards a

358 net cleavage of sucrose. Some uncertainties in flux calculations might be attributed to the
359 assumptions required to solve the model (flux minimization).

360

361 **5 Discussion**

362 *5.1 Three different fruit growth phases with their particular proteome and metabolic profile*

363 In banana, the growth pattern is cultivar dependent and fertilization influences the growth and
364 the shape of the fruit (Simmonds, 1953). A sigmoid type of growth has been described before in
365 a triploid banana with a B (balbisiana) genome (Awak legor) (Simmonds, 1953). The first period
366 of fast growth is characterized by cell division and cell elongation, while the second one is due to
367 cell elongation only (Ram et al., 1962). The increase in cell number in the initiating region of the
368 pulp has been reported to continue up to about 4 WAE in the cultivar Pisang lilin (a partenocarp
369 AA) (Ram et al., 1962). We did find evidence to confirm the involvement of cell division in
370 growth in our proteomics data. Histones are one of the primary components of chromatin and are
371 synthesized during the S-phase. The speed of DNA replication is depending on the rate of
372 histone biosynthesis (Ma et al., 2015).

373 Banana pulp tissue is a starch synthesizing sink tissue that needs to get all its energy from the
374 sucrose unloaded from the phloem and from starch degradation. From tomato, it is known that
375 the fruit growth consists of two phases: (i) a period of rapid fruit growth where sucrose synthase
376 is determining the sink strength, and (ii) a phase after rapid growth has ceased, where invertase
377 takes over (Nguyen-Quoc and Foyer, 2001). Based on the observed abundance pattern of
378 Sucrose Synthase (SuSy) and invertase, we hypothesize that the first fast growth phase is
379 completely dominated by Sucrose Synthase (SuSy), while the second fast growth phase is
380 dominated by invertase. The abundance of invertase showed an excellent correlation with the
381 growth rate (Figure 3).

382

383 *5.2 Starch synthesis: cytosolic glucose -6 phosphate and fructose are important sources for 384 starch synthesis*

385 Because starch synthesis in pulp is confined to amyloplasts, it relies entirely on translocation of
386 metabolites from the cytosol through the amyloplast envelope. The form in which carbon enters
387 the amyloplast has long been a matter of debate (Hofius and Börnke, 2007). The triose phosphate
388 transporter from chloroplasts is a perfectly annotated and studied transporter in the plastid

389 envelope of many plants. However, there is discussion as to whether the genes are expressed in
390 non-green tissue (Tobias et al., 1992; Neuhaus and Emes, 2000). In potato it is clear that triose
391 phosphate is not the substrate taken up to support starch synthesis (Hofius and Börnke, 2007).
392 Our data also point into the same direction since we were not able to identify a triose phosphate
393 transporter protein in plantain pulp. Amyloplasts of tubers or fruits are also normally not able to
394 generate hexose phosphates from C3 compounds due to the absence of fructose 1,6-
395 biphosphatase activity (Nguyen-Quoc and Foyer, 2001; Hofius and Börnke, 2007). They rely on
396 the import of cytosolically generated hexose phosphates as the source of carbon for starch
397 biosynthesis (Entwistle and Rees, 1988; Hofius and Börnke, 2007). This seems also to be the
398 case here in plantain since we were not able to identify a fructose 1,6-biphosphatase protein
399 during the period of investigation. The enzyme does seem active though in non-photosynthetic
400 tissues where it controls the rate of F6P production in the gluconeogenic pathway (Hofius and
401 Börnke, 2007). We did identify the enzyme though in low quantities in our previous analysis
402 where we analyzed ripening detached fruits (Bhuiyan et al., 2020). So also in our case it might
403 play a role in the starch breakdown much later when the ripening and sugar synthesis is more
404 advanced. None of the three predicted adenine nucleotide BT1 transporters (Ma10_p26970,
405 Ma07_p09880, Ma06_p06780) that transport ADP-glucose across the plastid membrane was
406 identified in the present study. Therefore, it is also unlikely that ADP-glucose is moving across
407 the amyloplast envelope to provide substrates for starch synthesis. We suggest that in plantain
408 banana the cytosolic glucose -6 phosphate is an important direct source of sugar for starch
409 synthesis as it is the case in maize (Tobias et al., 1992). This was confirmed by the high
410 abundance of the glucose-6-phosphate/phosphate translocator (6), phosphoglucomutase (5) and
411 the glucose-1-phosphate adenylyltransferase (2) (Table 3). We did identify a so far
412 uncharacterized sugar translocator (11) (Ma10_p26490) that has an almost perfect correlation
413 ($p < 0.0001$, $R = 0.99$) with SuSy (1) (Table 3, Figure 5). Plastids are able to transport sugars across
414 their membranes (Patzke et al., 2019). However, only two plastidic sugar transporters are well
415 known and described (Weber et al., 2000; Niittylä et al., 2004). These transporters reside in the
416 inner envelope membrane and respectively mediate the export of maltose and glucose
417 (Cordenunsi-Lysenko et al., 2019). Considering our observed tight correlation with SuSy, we
418 hypothesize that the Ma10_p26490.1 transporter transports fructose across the amyloplast
419 membrane. The abundance pattern of the plastidic fructokinase (12) corroborates this hypothesis

420 (Table 3, Figure 6A). Since only very few reports are available on plastid
421 fructose/glucose/sucrose H transporters (Patzke et al., 2019), more studies are needed to confirm
422 our hypothesis and confirm its physiological role in starch synthesis.

423 The soluble starch synthase (10) decreased in abundance during the further development while
424 granule bound starch synthase raised in abundance (9) (Table 3). This abundance pattern
425 suggests that during the early starch synthesis, soluble starch synthase is more important. The
426 fact that the polymerizing reactions of starch synthesis are not dominant in the control of starch
427 accumulation has to do with the balance between sink strength, starch synthesis and starch
428 breakdown and has been observed before (Tetlow et al., 2004). So based on the ANOVA
429 analysis and the correlations, the main drivers of starch synthesis in plantain pulp seem to be
430 Sucrose Synthase (1), Glucose-1-phosphate adenylyltransferase (ADP-glucose
431 pyrophosphorylase (AGPase)) (8), ADP,ATP carrier protein (19) and the so far uncharacterized
432 membrane sugar transporter (11) (Figure 6A, Table 3).

433

434 *5.3 Starch breakdown: phosphoglucan water dikinase, alpha-1,4 glucan phosphorylase,*
435 *phosphoglucan phosphatase, isoamylase and 4-alpha-glucanotransferase initiate breakdown.*

436

437 The starch-to-sucrose metabolism has been extensively studied in model systems in the context
438 of energy sources for plant growth and development (Streb and Zeeman, 2012). However, the
439 starch breakdown in fleshy fruits such as bananas is less understood (Cordenunsi-Lysenko et al.,
440 2019). All the genes involved in starch breakdown have been mapped on the banana genome
441 (Xiao et al., 2018). Based on what is known from Arabidopsis, it was hypothesized that in
442 banana starch-phosphorylating enzymes, termed glucan water dikinase (GWD), phosphorylate
443 the C6 position and the phosphoglucan water dikinase (PWD) phosphorylate the C3 position of
444 the glycosyl residues in starch (Cordenunsi-Lysenko et al., 2019). The role of phosphorylases
445 including GWD and PWD in starch breakdown during banana ripening is less understood, but
446 phosphorylation at the C3 and C6 position of the glucosyl residues in the starch of freshly
447 harvested unripe bananas has already been found, as well as the presence of PWD and GWD
448 (Cordenunsi-Lysenko et al., 2019). The steric hindrance of these phosphorylated groups alters
449 the organization of the granule and it has been hypothesized that PWD acts downstream of GWD
450 and that the induced phosphorylation of banana starch favors granule hydration and phase

451 transition from the crystalline state to the soluble state (Cordenunsi-Lysenko et al., 2019). Our
452 data confirm that dikinases play a role in early starch breakdown but not that PWD would act
453 downstream of GWD. We have identified the sole PWD protein present in the banana genome
454 (21) (Ma09_p07100.1;Mba09_g06570.1) as being present at the early stage of starch breakdown
455 process and being significantly upregulated (Table 3) while none of the two GWD proteins could
456 be detected. We did identify GWD1 in our previous study during the ripening of detached
457 plantain fruits (Bhuiyan et al., 2020) and also Xiao and coworkers identified GWD1 in ripening
458 detached fruits as being expressed at the late ripening stages (Xiao et al., 2018).

459 Phosphorolytic cleavage seems to be one of the first starch breakdown reactions. This hypothesis
460 is corroborated by the abundance profiles of phosphorylase (20) and from the glucose-6P
461 transporter (6) (Table 3, Figure 6B). The increase in abundance and activity of phosphorylase
462 was also observed when investigating phosphorylase during maturation and ripening (Da Mota et
463 al., 2002). Also other enzymes appear to contribute to the early degradation of starch.
464 Phosphoglucan phosphatases (22), α -1,6-glucosidase starch debranching enzyme (DBE) (23) and
465 4- α -glucanotransferase Disproportionating enzymes (DPE) (24) increase significantly in
466 abundance (Table 3, Figure 6B). We also observed the increased abundance of the plastidic
467 glucose transporter (25) (Table 3, Figure 6B), while the Maltose transporter, Maltose Excess
468 Protein transporter was not detected. Since also neither alpha nor beta-amylases were detected at
469 this early stage of ripening, we hypothesize that they act later in the ripening process. While
470 investigating detached ripening fruits, we found that plastidic alpha amylase acts before beta
471 amylase (Bhuiyan et al., 2020). This was also found by (Purgatto et al., 2001). Beta amylase is
472 essential to complete the breakdown and its upregulation was reported to be correlated to a
473 decrease in starch during fruit ripening (Purgatto et al., 2001; Bhuiyan et al., 2020)

474

475 *5.4 Sucrose synthesis: competition between vacuolar storage and recycling sucrose for growth*
476 *and starch resynthesis*

477 Starch breakdown products G1P and glucose are produced which can be metabolized further.
478 The cytoplasmic G1P has been proven to flow to the production of UGP-glucose (Figure 6B).
479 UGP-glucose can lead to sucrose synthesis either through SuSy (1), which is still abundantly
480 present, or through sucrose-phosphate synthase (27) which has its highest abundance at 12 WAE
481 (Table 3, Figure 6B). We did not confidently identify sucrose phosphatase at this early stage of

482 ripening. Only one peptide was found with low confidence. The reason for the low confidence is
483 probably the low abundance of the enzyme. We did confidently identify sucrose phosphatase in
484 our study of detached ripening fruits; it proved to be low abundant and was significantly
485 upregulated in the very late ripening stages (Bhuiyan et al., 2020). The formed sucrose can then
486 be transported to the vacuole for storage or further processing or can be degraded by invertase
487 (29) and/or SuSy (1) (Table 3, Figure 6B). Most banana production, both of dessert and cooking
488 types, is based on triploid cultivars. Banana cultivars are natural combinations of different A
489 (*acuminata*) and B (*balbisiana*) genomes and have been fixed over hundreds of years of human
490 selection. Plantain is an allopolyploid crop with an AAB genome (Carreel et al., 2002). Invertase
491 (29) Mba10_g13890.1, is only encoded on the B genome. The cytoplasmatic homologue coded
492 on the *acuminata* genome is most probably not or expressed in a very low level since we did not
493 find a confident specific spectrum. We have shown before that invertase is more abundant in
494 plantain compared with a Cavendish type (Bhuiyan et al., 2020). A higher invertase activity in
495 cooking bananas has already been associated with a changed sucrose/(glucose + fructose) ratio
496 (Fils-Lycaon et al., 2011). The breakdown of sucrose in the cytoplasm by invertase would enable
497 to flow back to starch synthesis and glycolysis to support further growth as discussed above
498 (Figure 3). Plantains are indeed a lot bigger than dessert bananas and contain much more starch.
499 Part of the metabolized sucrose is most likely also transported to the vacuole since we have
500 identified a monosaccharide transporter (30) (Ma04_p22640.1;Mba04_g23280.1) that has the
501 highest abundance at 12 WAE (Table 3, Figure 6B). Also the upregulation of the vacuolar
502 pyrophosphate energized proton pump (28) (Ma07_p22370.1) (Table 3) facilitates the transport
503 of sugars across the vacuolar membrane (Maeshima, 2000). Alterations in PPI metabolism have a
504 strong effect on sugar metabolism in which higher PPI levels increase starch accumulation and
505 decrease the level of sucrose. Decreased PPI levels have been associated with lower starch
506 biosynthetic rates (Osorio et al., 2013). The overexpression of a pyrophosphatase in tomato
507 resulted in an increase in the major sugars, a decrease in starch and an increase in vitamin C
508 (ascorbic acid) (Osorio et al., 2013). We have observed an increased abundance of soluble
509 inorganic pyrophosphatase, in the amyloplast (26) and at the vacuole (28) that coincides with the
510 decrease in starch synthesis and increase in sugars. (Tables 2, 3, Figure 6B). Indeed also proteins
511 involved in ascorbate synthesis (GDP-mannose 3,5-epimerase) and anti-oxidant defense
512 (ascorbate peroxidase, Monodehydroascorbate reductase) were higher abundant at 12 WAE

513 (Table 4). Ascorbic acid is also a cofactor of 1-aminocyclopropane-1-carboxylic acid oxidase
514 (ACO) that catalyzes the final step in the biosynthesis of the plant hormone ethylene (Smith et
515 al., 1992).

516

517 *5.5 Cultivar specific ethylene biosynthesis and auxin scavenging*

518 Climacteric fruits show a dramatic increase in the rate of respiration during ripening and this is
519 referred to as the climacteric rise (Paul et al., 2012). The rise in respiration is logarithmic and
520 occurs either simultaneously with the rise in ethylene production or it follows soon afterwards
521 (Burg, 1962). However, this large change in the magnitude of ethylene production can be
522 misleading. The important point is when the tissue becomes more sensitive to ethylene and
523 internal concentration reaches a threshold concentration required to induce biological responses
524 (Paul et al., 2012). Thus, ethylene plays a major role in the ripening process of climacteric fruits.
525 Climacteric fruits can ripen fully if they are harvested at completion of their growth period. We
526 finish our analysis at this point since this is the point that plantains are harvested and consumed.
527 The increase in sucrose production in time is significantly correlated to 1-aminocyclopropane-1-
528 carboxylate oxidase (ACO) (Table 4). ACO is the enzyme that produces ethylene. It is well-
529 known that banana is a climacteric fruit and so that ripening and net sugar synthesis starts upon
530 ethylene production (Cordenunsi and Lajolo, 1995; do Nascimento et al., 2000; Cordenunsi-
531 Lysenko et al., 2019). Banana has two interconnected feedback loops (Lü et al., 2018). The first
532 one is a positive feedback loop dependent on NAC transcription factors, while the second one is
533 controlled by MADS transcription factors and is able to maintain the ethylene synthesis even
534 when the first loop is blocked. It has been shown that banana ACO has a NAC motif in the
535 promoter sequence (Lü et al., 2018). It has been illustrated that ripening is a highly coordinated
536 process regulated at the transcript level (Kuang et al., 2021). We see a cultivar specific
537 interaction between cultivar and WAE meaning that the abundance of ACO changes differently
538 over time in both cultivars (Table 4). The disappearance of the large stock of starch in favour of
539 the accumulation of soluble sugars has also already been proven to contribute to pulp softening
540 (Shiga et al., 2011). A pectinesterase related protein and a lichenase are associated to pulp
541 softening (Li et al., 2019; Bhuiyan et al., 2020) and were correlated to both sugar and ACO
542 (Table 4). Proteins with sequence similarity to germins have been identified in various plant
543 species. Those ‘germin-like proteins’ (GLPs) have a global low sequence identity with germins

544 and constitute a large and highly diverse family with diverse functions among them auxin
545 binding (Bernier and Berna, 2001). Two auxin correlated GLPs were isolated in plum that were
546 correlated to the change of levels of autocatalytic ethylene levels and associated ripening (El-
547 Sharkawy et al., 2010). The authors found differential expression in two contrasting cultivars and
548 hypothesized that the differential endogenous auxin levels in the two cultivars change the levels
549 of available ethylene and so the ripening phenotype. We did find a GLP (Germin-like protein 12-
550 1) protein that has a significant correlation with ACO (Table 4). A prosite scan shows that the
551 protein has a Fe(2⁺) 2-oxoglutarate dioxygenase domain profile. A 2-oxoglutarate-dependent-Fe
552 (2⁺) dioxygenase in rice has been shown to convert active auxin (indole acetic acid) into
553 biologically inactive 2-oxoindole-3-acetic acid, supporting a key role in auxin catabolism (Zhao
554 et al., 2013). The protein has moreover also a cultivar specific pattern associated to the earlier
555 ripening Agbagba cultivar (Table 4). We hypothesize that this GLP/2-oxoglutarate dioxygenase
556 would catabolize auxin and hence stimulate ripening. In banana it has been proven that ethylene
557 promotes ripening and auxins delay it (Purgatto et al., 2001; Mainardi et al., 2006; Kuang et al.,
558 2021). Also in papaya the same has been proven (Zhang et al., 2020).

559 In plum, it has been shown that ethylene was a crucial factor affecting overall sugar metabolism
560 (Farcuh et al., 2018). More specifically, ethylene reduced sucrose catabolism and induced
561 sucrose biosynthesis but inversely, stimulated sorbitol breakdown via increased sorbitol and
562 dehydrogenase decrease sorbitol biosynthesis via decreased sorbitol-6-phosphate-dehydrogenase.
563 Also here, we observed an excellent correlation between ACO and a sorbitol dehydrogenase,
564 which catabolize sorbitol into fructose (Fru) and glucose (Glu). Also here the cultivar Agbagba
565 has a significantly earlier response than Obino '1 Ewai (Table 4).

566

567 **6 Conclusions**

568 By combining proteomics and flux studies, we gain here unique insights into the order of
569 appearance and dominance of specific enzymes/fluxes involved in starch and sugar synthesis and
570 breakdown. Fluxes give a broader analysis of the metabolism. Despite fluxes are calculated in a
571 non-compartmented network, we showed that proteome data complemented by fluxes can give a
572 satisfactory picture of the dynamics of metabolism during fruit development. The maturation in
573 plantain is completed around 10 WAE, indicated by a net breakdown in starch. The import of
574 G6P into the amyloplast and possibly fructose are the main drivers of starch synthesis. The

575 soluble starch synthase likely plays a more important role in the starch synthesis during the early
576 fruit development while granule bound starch synthase most likely influences the starch at the
577 mature stage. For starch breakdown, mainly DPE and phosphorylase produce the first hexoses
578 for sugar synthesis and amylases come into play at a later stage in ripening. In plantain
579 cytoplasmic invertase seems to play an important role in the breakdown of sucrose to support
580 further growth. The data pointed towards an interplay between auxins and ethylene, controlling
581 the ripening process. Despite the fact that both plantain cultivars are extremely close genetically,
582 we did find significant differences in ripening. The earlier ripening in Agbagba might be related
583 to an earlier induction of the second ethylene system and a bigger scavenging of auxins. This
584 information contributes to a better understanding of fruit development and maturation in banana
585 and more specifically plantains.

586

587 *Acknowledgements*

588 The authors would like to thank Kusay Arat for the technical support at SYBIOMA, KU Leuven,
589 Belgium. We acknowledge USAID for the project AID-BFS-G-II-00002-11 Reviving the
590 plantain breeding program at IITA – International Institute for Tropical Agriculture. The authors
591 would furthermore like to thank all donors who supported this work through their contributions
592 to the CGIAR Fund (<http://www.cgiar.org/who-we-are/cgiar-fund/fund-donors-2/>), and in
593 particular to the CGIAR Research Program on Roots, Tubers and Bananas, and the PHENOME
594 (French ANR-11-INBS-0012) project for funding. The metabolite analyses were performed on
595 Bordeaux Metabolome facility.

596

597 The authors have declared no conflict of interest.

598 **Table Legends**

599

600 Table 1: Proteins linked to growth in plantain banana pulp

601 WAE: Weeks After Emergence

602 This table only displays the ANOVA p-values of the protein paralog with the lowest value. The
603 full list of significant protein paralogs can be seen in Table S1.

604

605 Table 2: Metabolite data of plantain banana pulp.

606 Homogeneous groups over time within the same metabolite are indicated by a letter.
607 $A < B < C < D < E$, Groups sharing a letter are not significantly different (Fisher test).

608 WAE: weeks after emergence

609 OB: Obino 'l Ewai

610 AG: Agbagba

611

612 Table 3: Proteins linked to starch and sugar metabolism and correlations to starch and sucrose in
613 plantain banana pulp. This table only displays the ANOVA p-values of the protein paralog with
614 the lowest value. The full list of significant protein paralogs can be seen in Table S1.

615 WAE: Weeks After Emergence

616 R: Pearson correlation coefficient. Correlations in bold are statistically significant $p < 0.05$. This
617 table is non redundant and only displays the most significant protein paralogs. The full list can be
618 seen in Table S1

619

620 Table 4: Proteins linked to Ethylene response and correlations to ACO in plantain banana pulp

621

622 WAE: Weeks After Emergence

623 R: Pearson correlation coefficient. Correlations in bold are statistically significant $p < 0.05$. This
624 table only displays the ANOVA p-values of the protein paralog with the lowest value. The full
625 list of significant protein paralogs can be seen in Table S1.

626

627

628

629 **Figure legends**

630 FIGURE 1: Principal Component Analysis of the proteomics data (2183 proteins) of the two
631 varieties of plantain banana during fruit development. Displayed are the average scores per
632 cultivar and time point. Agbagba (blue) and Obino l'Ewai (red). The size of the data points is
633 proportional to the time of sampling. Pulp samples were analyzed at 6, 8, 10 and 12 WAE, $n = 3-$
634 5.

635

636 FIGURE 2: Changes in growth of fruit of two plantain varieties from 2 to 12 WAE (derivative of

637 cubic regression model). AG: Agbaba (Blue); OB: Obino l'ewai (Red).

638

639 FIGURE 3: Correlation between the average growth rate (6-12 WAE) and the average
640 normalized abundance of cytoplasmic invertase Mba10_g13890.1 for two plantain varieties.
641 Agbaba (blue); Obino l'ewai (red).

642

643 FIGURE 4: Changes in starch (derivative quadratic regression model). Samples harvested at 2, 4,
644 6, 8, 10 and 12 WAE. n =4-5 Agbaba (blue); Obino l'ewai (red) Net starch breakdown and so the
645 end of maturation is estimated to take place at 9.3 and 10.2 WAE for Agbaba and Obino l'ewai,
646 respectively.

647

648 FIGURE 5: Correlation between plastidic membrane transporter (11, Ma10_p26490) and SuSy
649 (1, Ma08_p23180) abundances. Samples have been harvested at 6, 8, 10 and 12 WAE. Agbaba
650 (blue); Obino l'ewai (red).

651

652 FIGURE 6A: Net starch synthesis at 6 WAE based on proteomic data in two plantain varieties.
653 Enzyme numbers in bold are significantly higher abundant at 6WAE (Table 3). The net direction
654 of the flux is indicated by an arrow. Enzymes and arrows in green have been confirmed by the
655 calculated fluxes (average of two cultivars). The size of the arrow indicates the protein
656 abundance (EMPAI). Grey arrows indicate unidentified or unsure proteins.

657 FIGURE 6B: Net starch breakdown at 12WAE. Enzymes in bold are significantly higher
658 abundant at 12WAE (Table 3). The net direction of the flux is indicated by an arrow. Enzymes
659 and arrows in green have been confirmed by the calculated fluxes (average of two cultivars).
660 The size of the arrow indicates the protein abundance (EMPAI). Grey arrows indicate unknown
661 or unsure proteins.

662

663 1: Sucrose synthase, 2: UTP-glucose-1-phosphate uridylyltransferase, 3: Fructokinase, 4:
664 Glucose-6-phosphate isomerase, cytosolic, 5: Phosphoglucomutase, 6: Glucose-6-
665 phosphate/phosphate translocator , chloroplastic, 7: Phosphoglucomutase, chloroplastic, 8:
666 Glucose-1-phosphate adenylyltransferase large subunit 2, chloroplastic, 9: Granule-bound starch
667 synthase , chloroplastic/amyloplastic, 10: Soluble starch synthase , chloroplastic/amyloplastic,

668 11: D-xylose-proton symporter-like 3, chloroplastic, 12: fructokinase, 13: Glucose-6-phosphate
669 isomerase 14: ATP-dependent 6-phosphofructokinase, 15: Pyrophosphate--fructose 6-phosphate
670 1-phosphotransferase subunit beta, 16: Fructose-bisphosphate aldolase, 17: Triosephosphate
671 isomerase, cytosolic, 18: Glyceraldehyde-3-phosphate dehydrogenase, cytosolic, 19: ADP,ATP
672 carrier protein , chloroplastic, 20: Alpha-1,4 glucan phosphorylase L isozyme,
673 chloroplastic/amyloplastic, 21: Phosphoglucan, water dikinase, chloroplastic, 22: Phosphoglucan
674 phosphatase LSF1, chloroplastic, 23: Isoamylase 3, chloroplastic, 24: 4-alpha-glucanotransferase
675 disproportioning enzyme, 25: Plastidic glucose transporter, 26: Soluble inorganic
676 pyrophosphatase, chloroplastic, 27: Sucrose-phosphate synthase, 28: Pyrophosphate-energized
677 vacuolar membrane proton pump, 29: Invertase, 30: Monosaccharide-sensing protein; 31:
678 Invertase; 32: Sucrose-phosphatase (identification unsure, only 1 peptide)

679

680 Figure 7: Simplified flux map, based on constrain-based modelling for Agbaba plantain cultivar
681 at 2 WAE, showing a high activity for fluxes in glycolysis, TCA cycle and mostly respiration (in
682 red). The same trend was obtained for both cultivars (see Figure S3). The arrow width is
683 proportional to flux intensity.

684

685

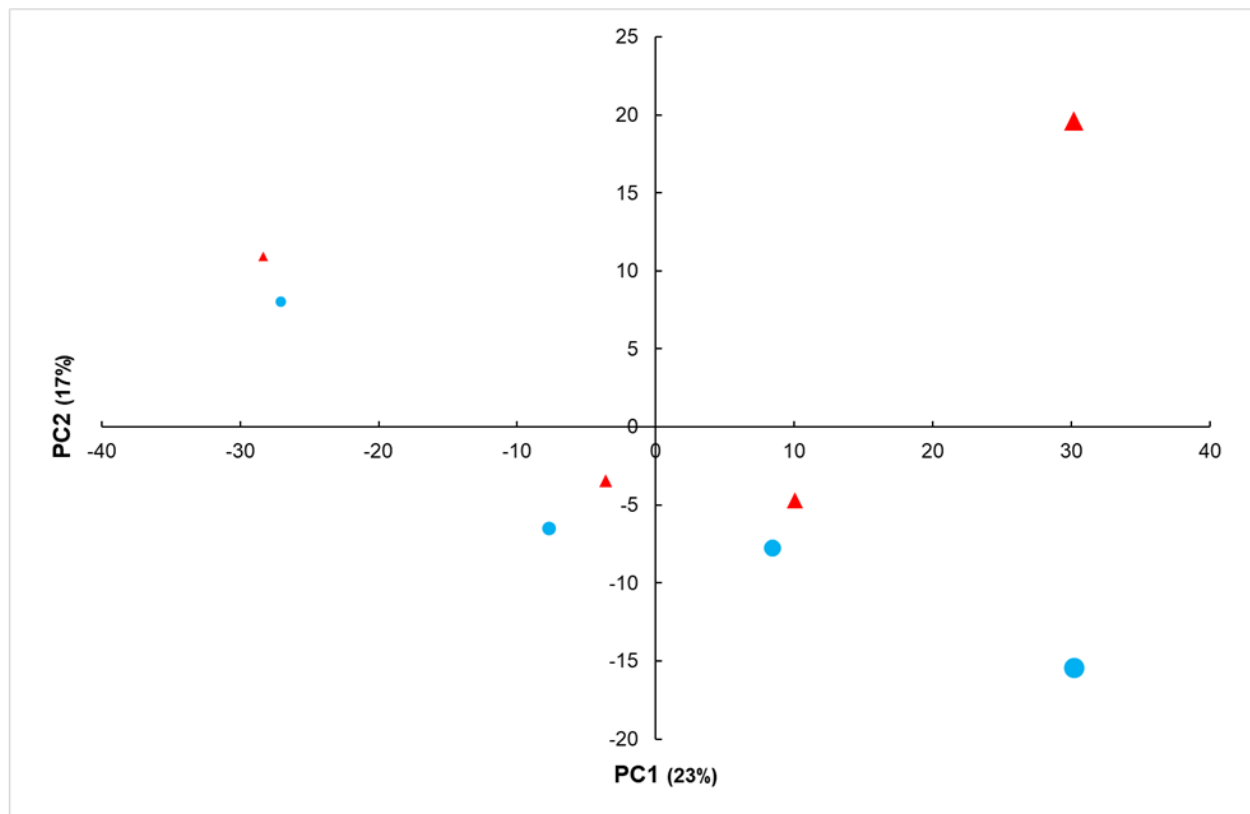
686 **References**

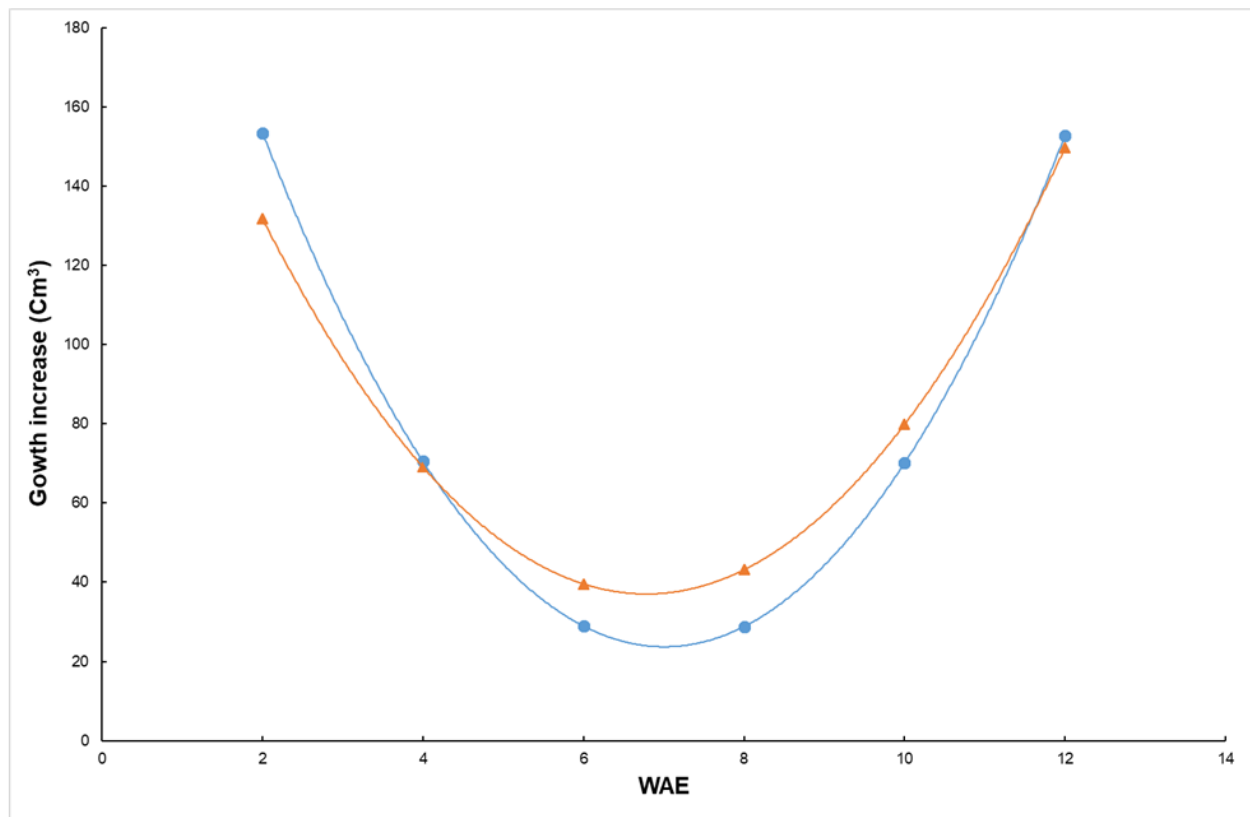
- 687 **Agopian RGD, Soares CA, Purgatto E, Cordenunsi BR, Lajolo FM** (2008) Identification of
688 fructooligosaccharides in different banana cultivars. *Journal of agricultural and food chemistry*
689 **56**: 3305-3310
- 690 **Almagro Armenteros JJ, Sønderby CK, Sønderby SK, Nielsen H, Winther O** (2017) DeepLoc: prediction
691 of protein subcellular localization using deep learning. *Bioinformatics* **33**: 3387-3395
- 692 **Asif MH, Lakhwani D, Pathak S, Gupta P, Bag SK, Nath P, Trivedi PK** (2014) Transcriptome analysis of
693 ripe and unripe fruit tissue of banana identifies major metabolic networks involved in fruit
694 ripening process. *BMC plant biology* **14**: 316
- 695 **Bantan-Polak T, Kassai M, Grant KB** (2001) A comparison of fluorescamine and naphthalene-2, 3-
696 dicarboxaldehyde fluorogenic reagents for microplate-based detection of amino acids. *Analytical*
697 *biochemistry* **297**: 128-136
- 698 **Bernier F, Berna A** (2001) Germins and germin-like proteins: plant do-all proteins. But what do they do
699 exactly? *Plant Physiology and Biochemistry* **39**: 545-554
- 700 **Bhuiyan F, Campos NA, Swennen R, Carpentier S** (2020) Characterizing fruit ripening in plantain and
701 Cavendish bananas: A proteomics approach. *Journal of Proteomics* **214**: 103632
- 702 **Blainski A, Lopes GC, De Mello JCP** (2013) Application and analysis of the folin ciocalteu method for the
703 determination of the total phenolic content from *Limonium brasiliense* L. *Molecules* **18**: 6852-
704 6865
- 705 **Bradford MM** (1976) A rapid and sensitive method for the quantitation of microgram quantities of
706 protein utilizing the principle of protein-dye binding. *Analytical biochemistry* **72**: 248-254
- 707 **Burg SP** (1962) The physiology of ethylene formation. *Annual Review of Plant Physiology* **13**: 265-302
- 708 **Buts K, Michielssens S, Hertog M, Hayakawa E, Cordewener J, America A, Nicolai B, Carpentier S** (2014)
709 Improving the identification rate of data independent label-free quantitative proteomics
710 experiments on non-model crops: A case study on apple fruit. *Journal of Proteomics* **105**: 31-45
- 711 **Campos NA, Swennen R, Carpentier SC** (2018) The Plantain Proteome, a Focus on Allele Specific
712 Proteins Obtained from Plantain Fruits. *Proteomics* **18**: 1700227
- 713 **Carpentier S, Dens K, Van den houwe I, Swennen R, Panis B** (2007) Lyophilization, a Practical Way to
714 Store and Transport Tissues Prior to Protein Extraction for 2DE Analysis? *Proteomics* **7**: 64-69
- 715 **Carpentier S, Witters E, Laukens K, Deckers P, Swennen R, Panis B** (2005) Preparation of protein
716 extracts from recalcitrant plant tissues: An evaluation of different methods for two-dimensional
717 gel electrophoresis analysis. *Proteomics* **5**: 2497-2507
- 718 **Carreel F, De Leon DG, Lagoda P, Lanaud C, Jenny C, Horry J-P, Du Montcel HT** (2002) Ascertaining
719 maternal and paternal lineage within *Musa* by chloroplast and mitochondrial DNA RFLP
720 analyses. *Genome* **45**: 679-692
- 721 **Colombié S, Beauvoit B, Nazaret C, Bénard C, Vercambre G, Le Gall S, Biais B, Cabasson C, Maucourt M,
722 Bernillon S** (2017) Respiration climacteric in tomato fruits elucidated by constraint-based
723 modelling. *New Phytologist* **213**: 1726-1739
- 724 **Colombié S, Nazaret C, Bénard C, Biais B, Mengin V, Solé M, Fouillen L, Dieuaide-Noubhani M, Mazat
725 JP, Beauvoit B** (2015) Modelling central metabolic fluxes by constraint-based optimization
726 reveals metabolic reprogramming of developing *Solanum lycopersicum* (tomato) fruit. *The Plant*
727 *Journal* **81**: 24-39
- 728 **Cordenunsi-Lysenko BR, Nascimento JRO, Castro-Alves VC, Purgatto E, Fabi JP, Peroni-Okyta FHG**
729 (2019) The starch is (not) just another brick in the wall: The primary metabolism of sugars during
730 banana ripening. *Frontiers in plant science* **10**
- 731 **Cordenunsi BR, Lajolo FM** (1995) Starch breakdown during banana ripening: sucrose synthase and
732 sucrose phosphate synthase. *Journal of agricultural and food chemistry* **43**: 347-351

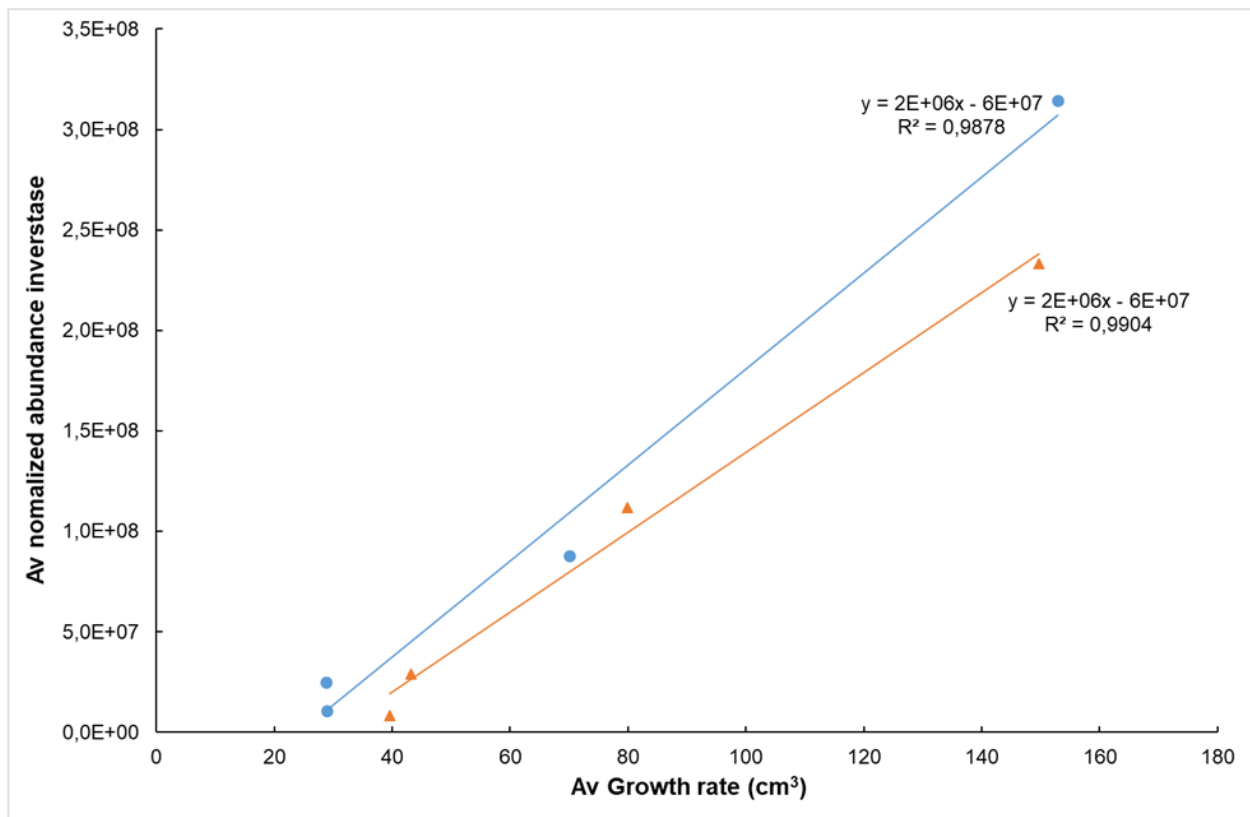
- 733 **Crouch H, Crouch J, Madsen S, Vuylsteke D, Ortiz R** (2000) Comparative analysis of phenotypic and
734 genotypic diversity among plantain landraces (*Musa* spp., AAB group). *Theoretical and Applied*
735 *Genetics* **101**: 1056-1065
- 736 **Da Mota RV, Cordenunsi BR, Do Nascimento JR, Purgatto E, Rosseto MR, Lajolo FM** (2002) Activity and
737 expression of banana starch phosphorylases during fruit development and ripening. *Planta* **216**:
738 325-333
- 739 **Dadzie B, Orchard J** (1997) Routine post-harvest screening of banana/plantain hybrids: criteria and
740 methods. INIBAP Technical Guidelines No. 2. *In*. INIBAP
- 741 **do Nascimento JRO, Cordenunsi BR, Lajolo FM** (2000) Sucrose synthase activity and expression during
742 development and ripening in bananas. *Journal of plant physiology* **156**: 605-611
- 743 **Droc G, Lariviere D, Guignon V, Yahiaoui N, This D, Garsmeur O, Dereeper A, Hamelin C, Argout X,**
744 **Dufayard J-F** (2013) The banana genome hub. *Database* **2013**
- 745 **Du L, Song J, Forney C, Palmer LC, Fillmore S, Zhang Z** (2016) Proteome changes in banana fruit peel
746 tissue in response to ethylene and high-temperature treatments. *Horticulture research* **3**: 1-12
- 747 **El-Sharkawy I, Mila I, Bouzayen M, Jayasankar S** (2010) Regulation of two germin-like protein genes
748 during plum fruit development. *Journal of experimental botany* **61**: 1761-1770
- 749 **Entwistle G, Rees T** (1988) Enzymic capacities of amyloplasts from wheat (*Triticum aestivum*)
750 endosperm. *Biochemical Journal* **255**: 391-396
- 751 **Farcuh M, Rivero RM, Sadka A, Blumwald E** (2018) Ethylene regulation of sugar metabolism in
752 climacteric and non-climacteric plums. *Postharvest Biology and Technology* **139**: 20-30
- 753 **Fils-Lycaon B, Julianus P, Chillet M, Galas C, Hubert O, Rinaldo D, Mbéguié-A-Mbéguié D** (2011) Acid
754 invertase as a serious candidate to control the balance sucrose versus (glucose+ fructose) of
755 banana fruit during ripening. *Scientia horticultrae* **129**: 197-206
- 756 **Gibon Y, Vigeolas H, Tiessen A, Geigenberger P, Stitt M** (2002) Sensitive and high throughput
757 metabolite assays for inorganic pyrophosphate, ADPGlc, nucleotide phosphates, and glycolytic
758 intermediates based on a novel enzymic cycling system. *The Plant Journal* **30**: 221-235
- 759 **Hawkins C, Ginzburg D, Zhao K, Dwyer W, Xue B, Xu A, Rice S, Cole B, Paley S, Karp P** (2021) Plant
760 Metabolic Network 15: A resource of genome-wide metabolism databases for 126 plants and
761 algae. *Journal of Integrative Plant Biology*
- 762 **Hendriks JH, Kolbe A, Gibon Y, Stitt M, Geigenberger P** (2003) ADP-glucose pyrophosphorylase is
763 activated by posttranslational redox-modification in response to light and to sugars in leaves of
764 *Arabidopsis* and other plant species. *Plant physiology* **133**: 838-849
- 765 **Hofius D, Börnke FA** (2007) Photosynthesis, carbohydrate metabolism and source–sink relations. *In*
766 *Potato biology and biotechnology*. Elsevier, pp 257-285
- 767 **Keller A, Nesvizhskii A, Kolker E, Aebersold R** (2002) An explanation of the Peptide Prophet algorithm
768 developed. *Anal. Chem* **74**: 5383-5392
- 769 **Kuang JF, Wu CJ, Guo YF, Walther D, Shan W, Chen JY, Chen L, Lu WJ** (2021) Deciphering transcriptional
770 regulators of banana fruit ripening by regulatory network analysis. *Plant biotechnology journal*
771 **19**: 477-489
- 772 **Li T, Yun Z, Wu Q, Qu H, Duan X, Jiang Y** (2019) Combination of Transcriptomic, Proteomic, and
773 Metabolomic Analysis Reveals the Ripening Mechanism of Banana Pulp. *Biomolecules* **9**: 523
- 774 **Lü P, Yu S, Zhu N, Chen Y-R, Zhou B, Pan Y, Tzeng D, Fabi JP, Argyris J, Garcia-Mas J** (2018) Genome
775 encode analyses reveal the basis of convergent evolution of fleshy fruit ripening. *Nature Plants*
776 **4**: 784-791
- 777 **Ma Y, Kanakousaki K, Buttitta L** (2015) How the cell cycle impacts chromatin architecture and influences
778 cell fate. *Frontiers in Genetics* **6**
- 779 **Maeshima M** (2000) Vacuolar H⁺-pyrophosphatase. *Biochimica et Biophysica Acta (BBA)-Biomembranes*
780 **1465**: 37-51

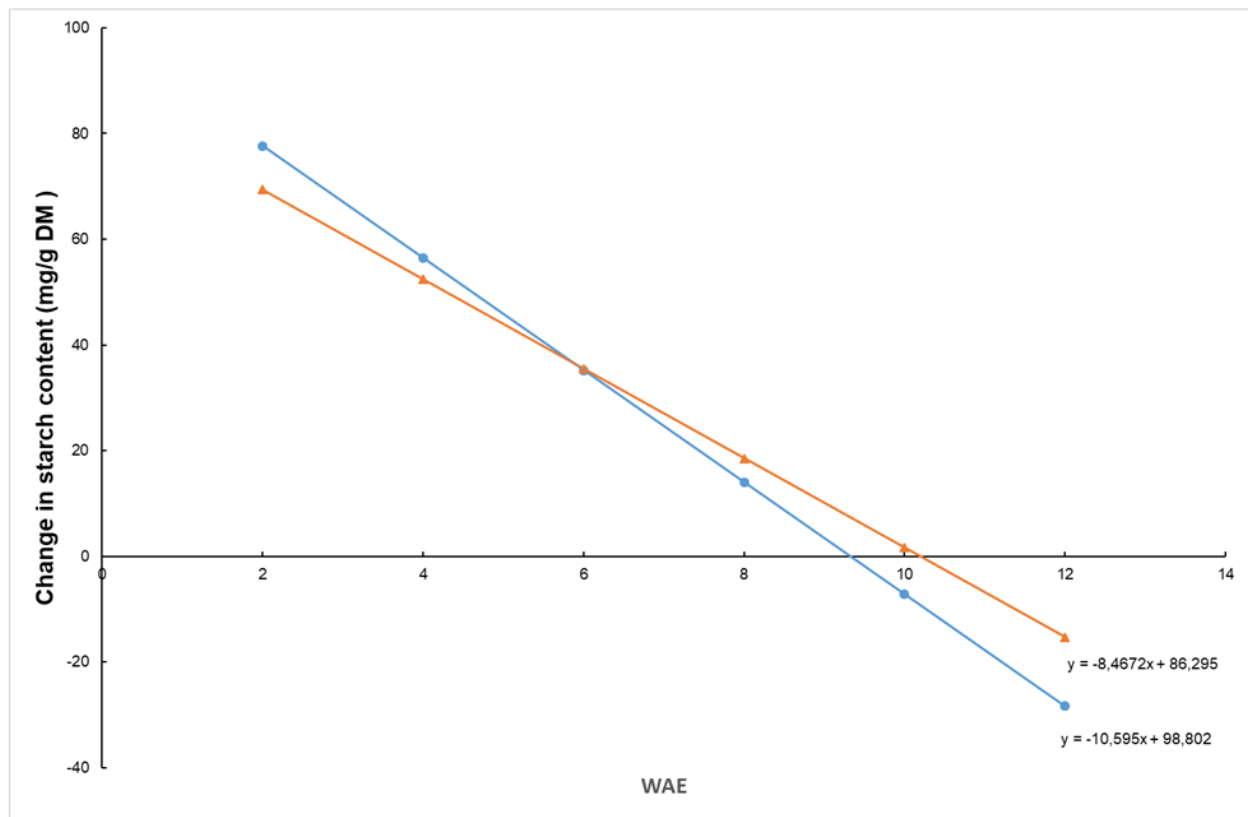
- 781 **Mainardi JA, Purgatto E, Vieira A, Bastos WA, Cordenunsi BR, Oliveira do Nascimento JR, Lajolo FM**
782 (2006) Effects of ethylene and 1-methylcyclopropene (1-MCP) on gene expression and activity
783 profile of α -1, 4-glucan-phosphorylase during banana ripening. *Journal of agricultural and food*
784 *chemistry* **54**: 7294-7299
- 785 **Martin G, Baurens F-C, Droc G, Rouard M, Cenci A, Kilian A, Hastie A, Doležel J, Aury J-M, Alberti A**
786 (2016) Improvement of the banana “*Musa acuminata*” reference sequence using NGS data and
787 semi-automated bioinformatics methods. *BMC genomics* **17**: 243
- 788 **Mollering H** (1985) L(-) malate. *In* HU Bergmeyer, ed, *Methods of enzymatic analysis*, Vol 7. VCH
789 Verlagsgesellschaft, Weinheim, Germany, pp 39-47
- 790 **Nesvizhskii AI, Keller A, Kolker E, Aebersold R** (2003) A statistical model for identifying proteins by
791 tandem mass spectrometry. *Analytical chemistry* **75**: 4646-4658
- 792 **Neuhaus H, Emes M** (2000) Nonphotosynthetic metabolism in plastids. *Annual review of plant biology*
793 **51**: 111-140
- 794 **Nguyen-Quoc B, Foyer CH** (2001) A role for ‘futile cycles’ involving invertase and sucrose synthase in
795 sucrose metabolism of tomato fruit. *Journal of Experimental Botany* **52**: 881-889
- 796 **Niittylä T, Messerli G, Trevisan M, Chen J, Smith AM, Zeeman SC** (2004) A previously unknown maltose
797 transporter essential for starch degradation in leaves. *Science* **303**: 87-89
- 798 **Orth JD, Thiele I, Pálsson BØ** (2010) What is flux balance analysis? *Nature biotechnology* **28**: 245-248
- 799 **Osorio S, Nunes-Nesi A, Stratmann M, Fernie A** (2013) Pyrophosphate levels strongly influence
800 ascorbate and starch content in tomato fruit. *Frontiers in plant science* **4**: 308
- 801 **Patzke K, Prananingrum P, Klemens PA, Trentmann O, Rodrigues CM, Keller I, Fernie AR, Geigenberger**
802 **P, Bölter B, Lehmann M** (2019) The plastidic sugar transporter pSuT influences flowering and
803 affects cold responses. *Plant physiology* **179**: 569-587
- 804 **Paul V, Pandey R, Srivastava GC** (2012) The fading distinctions between classical patterns of ripening in
805 climacteric and non-climacteric fruit and the ubiquity of ethylene—an overview. *Journal of Food*
806 *Science and Technology* **49**: 1-21
- 807 **Purgatto E, Lajolo FM, do Nascimento JRO, Cordenunsi BR** (2001) Inhibition of β -amylase activity, starch
808 degradation and sucrose formation by indole-3-acetic acid during banana ripening. *Planta* **212**:
809 823-828
- 810 **Ram HM, Ram M, Steward F** (1962) Growth and development of the banana plant: 3. A. The origin of
811 the inflorescence and the development of the flowers: B. The structure and development of the
812 fruit. *Annals of Botany* **26**: 657-673
- 813 **Rohart F, Gautier B, Singh A, Lê Cao K-A** (2017) mixOmics: An R package for ‘omics feature selection and
814 multiple data integration. *PLoS computational biology* **13**: e1005752
- 815 **Searle BC** (2010) Scaffold: a bioinformatic tool for validating MS/MS-based proteomic studies.
816 *Proteomics* **10**: 1265-1269
- 817 **Shiga TM, Soares CA, Nascimento JR, Purgatto E, Lajolo FM, Cordenunsi BR** (2011) Ripening-associated
818 changes in the amounts of starch and non-starch polysaccharides and their contributions to fruit
819 softening in three banana cultivars. *Journal of the Science of Food and Agriculture* **91**: 1511-
820 1516
- 821 **Simmonds NW** (1953) The development of the banana fruit. *Journal of Experimental Botany* **4**: 87-105
- 822 **Simmonds NW** (1962) *The evolution of the bananas*. Longmans, Green,, London
- 823 **Singh A, Shannon CP, Gautier B, Rohart F, Vacher M, Tebbutt SJ, Lê Cao K-A** (2019) DIABLO: an
824 integrative approach for identifying key molecular drivers from multi-omics assays.
825 *Bioinformatics* **35**: 3055-3062
- 826 **Smith JJ, Ververidis P, John P** (1992) Characterization of the ethylene-forming enzyme partially purified
827 from melon. *Phytochemistry* **31**: 1485-1494

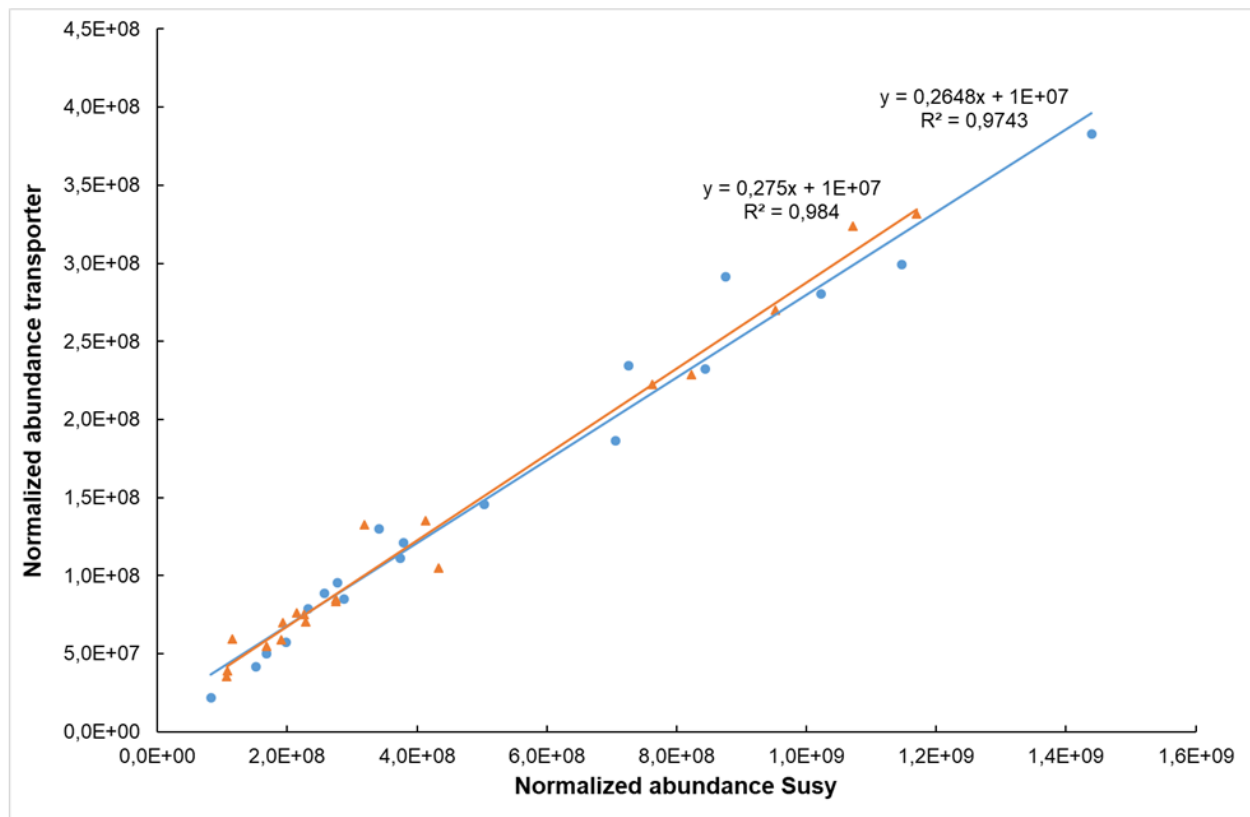
- 828 **Soares CA, Peroni-Okita FHGa, Cardoso MB, Shitakubo R, Lajolo FM, Cordenunsi BR** (2011) Plantain
829 and banana starches: granule structural characteristics explain the differences in their starch
830 degradation patterns. *Journal of Agricultural and Food Chemistry* **59**: 6672-6681
- 831 **Soubeyrand E, Colombié S, Beauvoit B, Dai Z, Cluzet S, Hilbert G, Renaud C, Maneta-Peyret L,**
832 **Dieuaide-Noubhani M, Méryllon J-M** (2018) Constraint-based modeling highlights cell energy,
833 redox status and α -ketoglutarate availability as metabolic drivers for anthocyanin accumulation
834 in grape cells under nitrogen limitation. *Frontiers in plant science* **9**: 421
- 835 **Stitt M, Lilley RM, Gerhardt R, Heldt HW** (1989) Metabolite levels in specific cells and subcellular
836 compartments of plant leaves. *Methods in enzymology* **174**: 518-552
- 837 **Streb S, Zeeman SC** (2012) Starch metabolism in Arabidopsis. *The Arabidopsis book/American Society of*
838 *Plant Biologists* **10**
- 839 **Tetlow IJ, Morell MK, Emes MJ** (2004) Recent developments in understanding the regulation of starch
840 metabolism in higher plants. *Journal of experimental botany* **55**: 2131-2145
- 841 **Tobias RB, Boyer CD, Shannon JC** (1992) Alterations in carbohydrate intermediates in the endosperm of
842 starch-deficient maize (*Zea mays* L.) genotypes. *Plant Physiology* **99**: 146-152
- 843 **Toledo TT, Nogueira SB, Cordenunsi BR, Gozzo FC, Pilau EJ, Lajolo FM, do Nascimento JRO** (2012)
844 Proteomic analysis of banana fruit reveals proteins that are differentially accumulated during
845 ripening. *Postharvest Biology and Technology* **70**: 51-58
- 846 **van Wesemael J, Hueber Y, Kissel E, Campos N, Swennen R, Carpentier S** (2018) Homeolog expression
847 analysis in an allotriploid non-model crop via integration of transcriptomics and proteomics.
848 *Scientific reports* **8**: 1353
- 849 **Vuylsteke D, Ortiz R, Pasberg-Gauhl C, Gauhl F, Gold C, Ferris S, Speijer P** (1993) Plantain and banana
850 research at the International Institute of Tropical Agriculture. *HortScience* **28**: 874-971
- 851 **Wang Z, Miao H, Liu J, Xu B, Yao X, Xu C, Zhao S, Fang X, Jia C, Wang J, Zhang J, Li J, Xu Y, Wang J, Ma**
852 **W, Wu Z, Yu L, Yang Y, Liu C, Guo Y, Sun S, Baurens F-C, Martin G, Salmon F, Garsmeur O,**
853 **Yahiaoui N, Hervouet C, Rouard M, Laboureau N, Habas R, Ricci S, Peng M, Guo A, Xie J, Li Y,**
854 **Ding Z, Yan Y, Tie W, D'Hont A, Hu W, Jin Z** (2019) *Musa balbisiana* genome reveals subgenome
855 evolution and functional divergence. *Nature Plants* **5**: 810-821
- 856 **Weber A, Servaites JC, Geiger DR, Kofler H, Hille D, Gröner F, Hebbeker U, Flügge U-I** (2000)
857 Identification, purification, and molecular cloning of a putative plastidic glucose translocator.
858 *The Plant Cell* **12**: 787-801
- 859 **White PJ** (2002) Recent advances in fruit development and ripening: an overview. *Journal of*
860 *Experimental Botany* **53**: 1995-2000
- 861 **Xiao Yy, Kuang Jf, Qi Xn, Ye Yj, Wu ZX, Chen Jy, Lu Wj** (2018) A comprehensive investigation of starch
862 degradation process and identification of a transcriptional activator Mab HLH 6 during banana
863 fruit ripening. *Plant biotechnology journal* **16**: 151-164
- 864 **Zhang T, Li W, Xie R, Xu L, Zhou Y, Li H, Yuan C, Zheng X, Xiao L, Liu K** (2020) CpARF2 and CpEIL1 interact
865 to mediate auxin–ethylene interaction and regulate fruit ripening in papaya. *The Plant Journal*
866 **103**: 1318-1337
- 867 **Zhao Z, Zhang Y, Liu X, Zhang X, Liu S, Yu X, Ren Y, Zheng X, Zhou K, Jiang L** (2013) A role for a
868 dioxygenase in auxin metabolism and reproductive development in rice. *Developmental Cell* **27**:
869 113-122
- 870



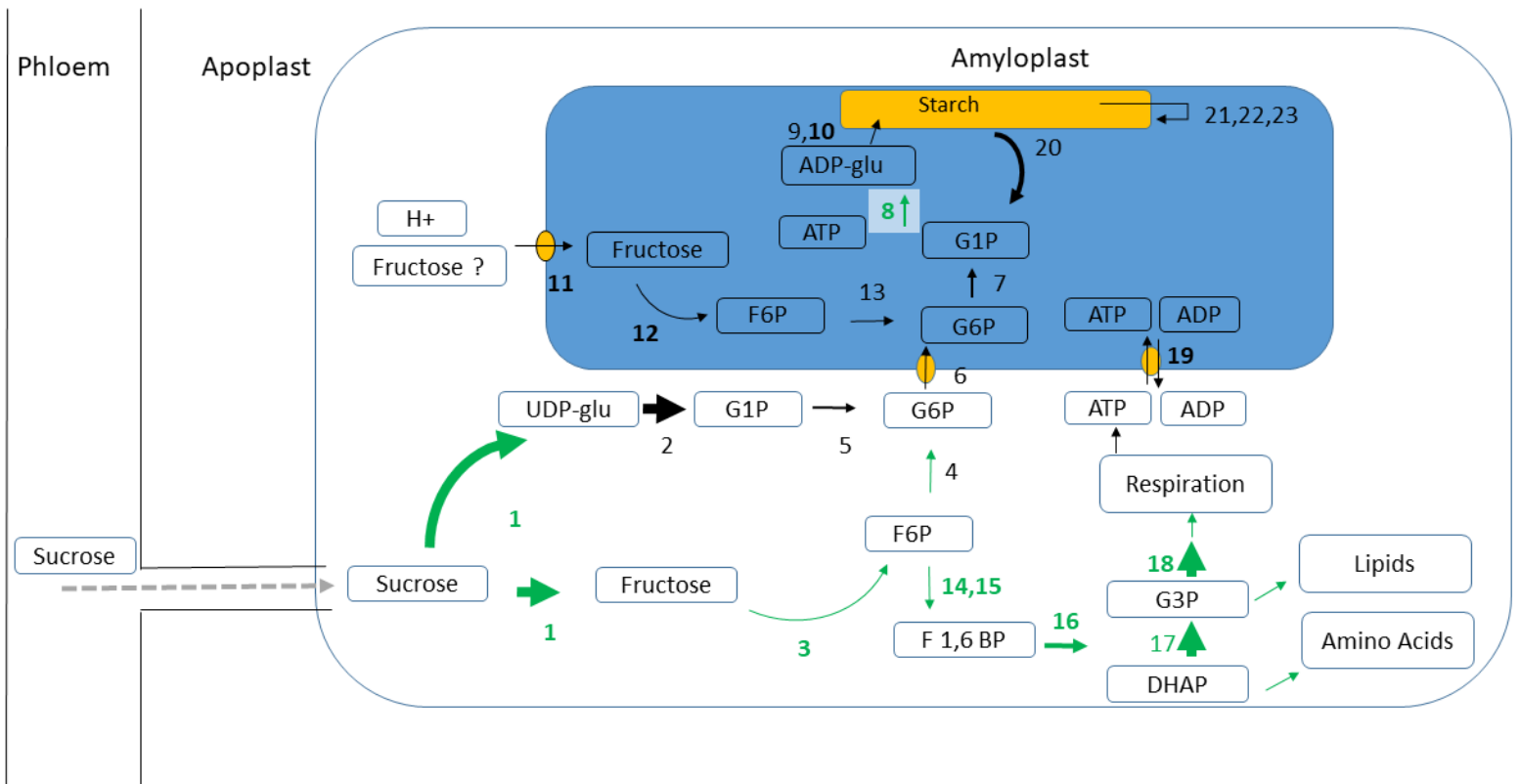




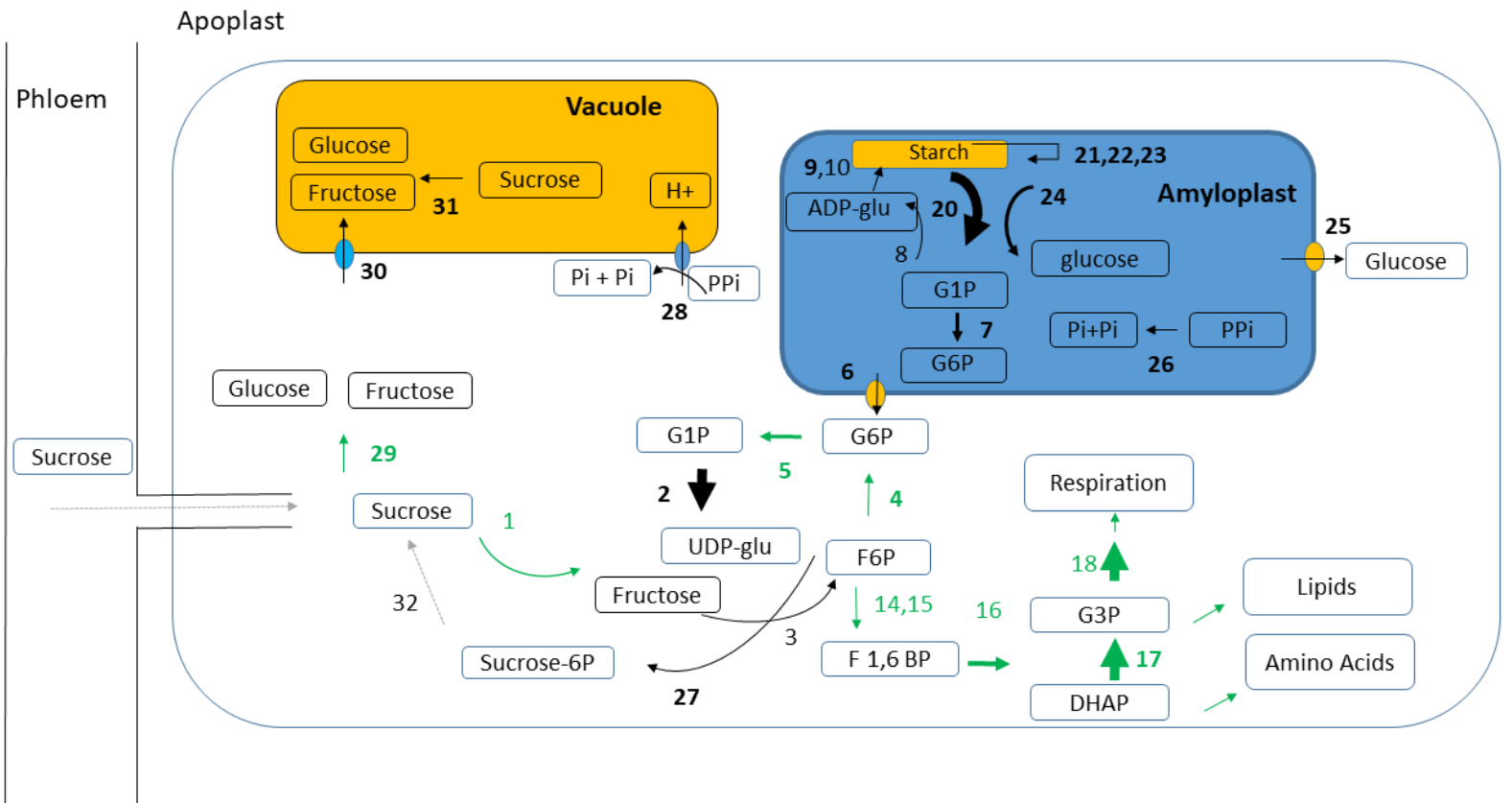


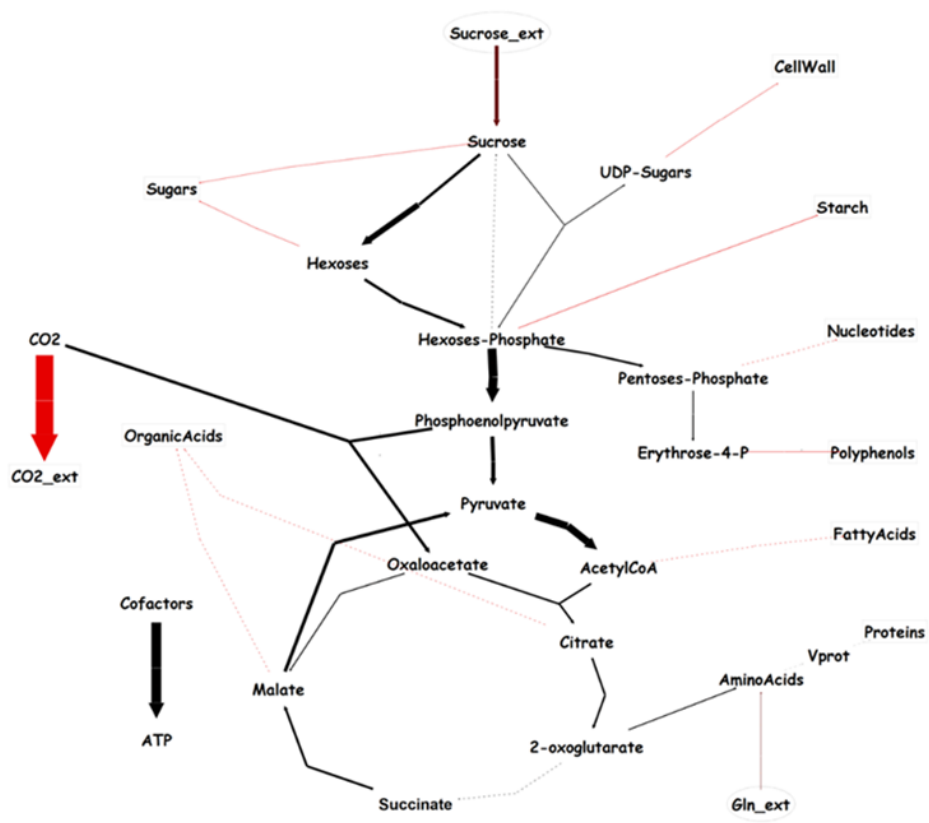


A



B





description	ANOVA p value			Peptides used for quantitation	max fold change	WAE	
	WAE	Genotype	WAE*Genotype			Highest mean condition	Lowest mean condition
26S protease regulatory subunit 7	0,00	0,87	0,94	6	1,7	6	12
26S proteasome non-ATPase regulatory subunit 1	0,00	0,01	0,01	7	2,9	6	12
26S proteasome regulatory subunit 6B homolog	0,00	0,07	0,01	11	2,2	6	12
40S ribosomal protein S11	0,00	0,92	0,45	8	3,0	6	12
40S ribosomal protein S13	0,00	0,89	0,72	4	1,9	6	10
40S ribosomal protein S14	0,00	0,40	0,79	9	3,2	6	12
40S ribosomal protein S16	0,00	0,73	0,53	10	1,6	6	10
40S ribosomal protein S18	0,00	0,13	0,03	14	1,8	6	12
40S ribosomal protein S19	0,00	0,21	0,80	11	2,4	6	12
40S ribosomal protein S24-2	0,00	0,54	0,54	3	3,7	6	12
40S ribosomal protein S25-4	0,00	0,62	0,53	6	1,8	6	12
40S ribosomal protein S26-1	0,00	0,08	0,70	3	2,0	6	12
40S ribosomal protein S3a	0,00	0,48	0,34	8	2,0	6	12
40S ribosomal protein S5 (Fragment)	0,00	0,06	0,32	7	2,5	6	12
40S ribosomal protein S9-2	0,00	0,69	0,86	10	1,7	6	10
40S ribosomal protein S9	0,00	0,75	0,17	8	3,5	6	12
50S ribosomal protein L12, chloroplastic	0,00	0,28	0,86	2	4,7	6	12
60S acidic ribosomal protein P2B	0,00	0,40	0,82	5	2,3	6	12
60S ribosomal protein L11	0,00	0,43	0,13	6	2,6	6	12
60S ribosomal protein L12	0,00	0,21	0,06	8	1,9	6	12
60S ribosomal protein L13-1	0,00	0,55	0,82	8	1,9	6	10
60S ribosomal protein L22-2	0,01	0,88	0,14	2	2,0	6	12
60S ribosomal protein L23	0,00	0,88	0,68	5	1,6	6	12
60S ribosomal protein L23A	0,00	0,03	0,79	8	3,0	6	12
60S ribosomal protein L30	0,00	0,97	0,58	2	2,3	6	12
60S ribosomal protein L34	0,01	0,69	0,45	5	2,5	6	12
60S ribosomal protein L35	0,00	0,65	0,87	6	2,6	6	12
60S ribosomal protein L35a-3	0,00	0,70	0,36	2	2,2	6	12
60S ribosomal protein L36-3	0,00	0,06	0,65	6	2,9	6	12
60S ribosomal protein L37a	0,00	0,46	0,79	2	10,8	6	12
60S ribosomal protein L4-1	0,00	0,49	0,40	13	2,9	6	12
60S ribosomal protein L6	0,00	0,42	0,60	7	2,1	6	10
60S ribosomal protein L7-2	0,00	0,75	0,11	7	2,1	6	12
60S ribosomal protein L9	0,00	0,57	0,00	6	2,4	6	12
Actin-depolymerizing factor 2	0,00	0,05	0,12	2	3,9	6	12
Beta-glucosidase 1	0,00	0,46	0,91	3	1,9	6	12
Eukaryotic initiation factor 4A-3	0,00	0,19	0,63	24	1,7	6	12
Eukaryotic translation initiation factor 3 subunit 1	0,00	0,61	0,62	3	4,9	6	12
Guanine nucleotide-binding protein subunit beta-1	0,00	0,13	0,14	11	2,6	6	12
Histone H2A.1	0,00	0,07	0,09	2	9,7	6	12
Histone H2B	0,00	0,00	0,28	2	2,4	6	12
Histone H2B.6	0,00	0,00	0,92	6	4,5	6	12
Histone H4	0,00	0,04	0,58	4	57,1	6	12
Proteasome subunit alpha type-1-A	0,00	0,84	0,54	8	1,7	6	12
Proteasome subunit alpha type-2-A	0,00	0,40	0,45	7	1,6	6	12
Proteasome subunit alpha type-5	0,00	0,13	0,51	16	3,0	6	12
Proteasome subunit alpha type-6	0,00	0,18	0,05	12	2,3	6	12
Proteasome subunit alpha type-7	0,00	0,05	0,05	7	1,8	6	12
Proteasome subunit beta type-4	0,00	0,26	0,77	5	4,1	6	10
Protein ASPARTIC PROTEASE IN GUARD CELL 1	0,00	0,25	0,83	8	3,6	6	10
T-complex protein 1 subunit epsilon	0,00	0,27	0,71	6	2,2	6	12
T-complex protein 1 subunit theta	0,00	0,55	0,04	8	3,0	6	12
UDP-glucose 6-dehydrogenase 4	0,00	0,13	0,02	5	3,0	6	12
UDP-glucuronic acid decarboxylase 6	0,00	0,90	0,66	6	2,0	6	10

time point WAE	2	4	6	8	10	12	2	4	6	8	10	12
Genotype	AG	AG	AG	AG	AG	AG	OL	OL	OL	OL	OL	OL
Biological replicates	5	5	5	5	5	4	5	5	5	5	5	4
	Mean $\mu\text{mol/gDW}$											
F6P	0,5 ^D	0,4 ^{ABCD}	0,3 ^{AB}	0,3 ^{AB}	0,3 ^{ABC}	0,5 ^{CD}	0,5 ^{CD}	0,4 ^{ABCD}	0,3 ^A	0,3 ^{AB}	0,4 ^{BCD}	0,4 ^{ABCD}
Fructose	82,7 ^C	51,5 ^{BC}	19,1 ^{AB}	9,5 ^A	12,1 ^A	9,7 ^A	40,1 ^{AB}	54,9 ^{BC}	9,2 ^A	8,3 ^A	7,6 ^A	4,1 ^A
G1P	0,4 ^C	0,3 ^{ABC}	0,1 ^A	0,2 ^{AB}	0,2 ^{ABC}	0,2 ^{AB}	0,3 ^{ABC}	0,3 ^{BC}	0,1 ^A	0,2 ^{AB}	0,2 ^A	0,2 ^{AB}
G6P	3,6 ^{BCDE}	2,6 ^{ABC}	2,2 ^A	2,5 ^{AB}	3,4 ^{BCDE}	4,5 ^E	4,1 ^{DE}	3,1 ^{ABCD}	2,9 ^{ABCD}	3,3 ^{ABCDE}	3,8 ^{CDE}	4,3 ^{DE}
Glucose	39,8 ^B	23,2 ^{AB}	6,3 ^A	4,2 ^A	4,4 ^{AB}	4,2 ^A	21,2 ^{AB}	21,8 ^{AB}	3,7 ^A	4,2 ^A	4,1 ^A	4,3 ^A
Starch	266,2 ^A	313,6 ^{ABC}	386,6 ^{ABCD}	410,2 ^{BCD}	457,4 ^D	442,7 ^{CD}	268,3 ^A	264,2 ^A	305,8 ^{AB}	423,3 ^{BCD}	449,1 ^D	434 ^{BCD}
Sucrose	92,1 ^{ABC}	67,0 ^{ABC}	75,5 ^{AB}	108,3 ^{BCD}	127,8 ^{CDE}	160,2 ^E	98,8 ^{ABC}	68,6 ^A	108,3 ^{BCD}	141,6 ^{DE}	156,1 ^E	148,7 ^{DE}

enzyme	description	ANOVA p value			Peptides used for quantitation	max fold change	Highest mean condition	Lowest mean condition	R	
		WAE	Genotype	DAF*Genotype					starch	sucrose
1	Sucrose synthase	0,00	0,03	0,59	10	8,2	6	12	-0,41	-0,68
2	UTP-glucose-1-phosphate uridylyltransferase	0,00	0,42	0,07	30	2,1	12	6	0,16	0,50
3	Fructokinase-1	0,00	0,26	0,83	9	2,0	6	12	-0,28	-0,56
4	Glucose-6-phosphate isomerase, cytosolic 1	0,00	0,05	0,19	12	9,0	12	6	0,21	0,44
5	phosphoglucosyltransferase, putative, expressed	0,06	0,47	0,55	7	8,2	12	8	0,12	0,21
6	Glucose-6-phosphate/phosphate translocator 2, chloroplast	0,00	0,55	0,45	5	3,0	12	6	0,02	0,29
7	Phosphoglucosyltransferase 2C chloroplast	0,00	0,40	0,94	24	1,9	12	6	0,21	0,60
8	Glucose-1-phosphate adenylyltransferase large subunit 2, chl	0,00	0,55	0,35	14	2,8	6	12	-0,43	-0,67
9	Granule-bound starch synthase 1, chloroplast/amyloplastic	0,02	0,65	0,45	4	2,4	12	6	0,27	0,23
10	Soluble starch synthase 3, chloroplast/amyloplastic	0,03	0,29	0,30	11	3,2	6	12	0,13	-0,34
11	D-xylose-proton symporter-like 3, chloroplast	0,00	0,06	0,58	4	6,2	6	12	-0,40	-0,67
12	Probable fructokinase-6, chloroplast	0,04	0,12	0,29	3	1,7	6	12	-0,03	-0,22
13	Glucose-6-phosphate isomerase 1, chloroplast	0,06	0,32	0,25	13	1,3	12	10	0,23	0,50
14	ATP-dependent 6-phosphofructokinase 3	0,01	0,45	0,51	5	1,5	6	12	-0,12	-0,53
15	Pyrophosphate-fructose 6-phosphate 1-phosphotransferase	0,00	0,42	0,78	4	2,0	6	10	-0,39	-0,52
16	Fructose-bisphosphate aldolase cytoplasmic isozyme	0,00	0,01	0,68	28	1,3	6	12	-0,27	-0,39
17	Triosephosphate isomerase, cytosolic	0,00	0,01	0,08	3	2,7	12	6	0,05	0,31
18	Glyceraldehyde-3-phosphate dehydrogenase 2, cytosolic	0,00	0,18	0,13	25	1,6	6	10	-0,39	-0,17
19	ADP/ATP carrier protein 1, chloroplast	0,00	0,23	0,03	3	72,7	6	12	-0,44	-0,57
20	Alpha-1,4 glucan phosphorylase L isozyme, chloroplast/amy	0,00	0,89	0,29	92	3,3	12	6	0,22	0,64
21	Phosphoglucan, water dikinase, chloroplast	0,00	0,57	0,99	28	3,5	12	6	0,15	0,52
22	Phosphoglucan phosphatase LSF1, chloroplast	0,00	0,26	0,96	6	1,8	12	6	0,03	0,43
23	Isoamylase 3, chloroplast	0,00	0,15	0,92	14	2,5	12	6	0,13	0,51
24	4-alpha-glucanotransferase	0,00	0,29	0,00	32	2,3	12	6	0,18	0,68
25	Plastidic glucose transporter	0,00	0,66	0,10	4	2,4	10	6	0,19	0,13
26	Soluble inorganic pyrophosphatase, chloroplast	0,00	0,29	0,17	7	3,3	12	6	0,12	0,34
27	Sucrose-phosphate synthase	0,01	0,93	0,90	25	2,0	12	6	0,15	0,45
28	Pyrophosphate-energized vacuolar membrane proton pump	0,00	0,05	0,23	20	5,6	12	6	0,21	0,46
29	Beta-fructofuranosidase 2C insoluble isoenzyme 3	0,00	0,54	0,42	17	37,3	12	6	0,11	0,41
30	Monosaccharide-sensing protein	0,00	0,69	0,91	3	9,7	12	6	0,20	0,50
31	Beta-fructofuranosidase, insoluble isoenzyme 3	0,00	0,82	0,82	5	19,5	12	6	0,11	0,41

Description	ANOVA p value			Peptides used for quantitation	max fold change	WAE		R	
	WAE	Genotype	WAE*Genotype			Highest mean condition	Lowest mean condition	sucrose	ACO
1-aminocyclopropane-1-carboxylate oxidase	0,00	0,30	0,03	39	19,1	12	6	0,60	1,00
Sorbitol dehydrogenase	0,00	0,42	0,02	13	3,4	12	6	0,63	0,91
Germin-like protein 12-1	0,00	0,06	0,00	5	123,8	12	6	0,58	0,88
Pectinesterase/pectinesterase inhibitor PPE8B	0,00	0,34	0,01	18	12,8	12	6	0,59	0,84
Putative Pectinesterase	0,00	0,86	0,39	11	7,1	12	6	0,57	0,82
L-ascorbate peroxidase, cytosolic	0,00	0,07	0,00	14	2,5	12	6	0,57	0,82
GDP-mannose 3,5-epimerase 1	0,00	0,21	0,56	13	1,9	12	6	0,50	0,82
Probable L-ascorbate peroxidase 7, chloroplastic	0,00	0,12	0,87	7	3,4	12	6	0,50	0,75
Lichenase	0,00	0,23	0,00	20	46,1	12	6	0,56	0,73

Parsed Citations

Agopian RGD, Soares CA, Purgatto E, Cordenunsi BR, Lajolo FM (2008) Identification of fructooligosaccharides in different banana cultivars. Journal of agricultural and food chemistry 56: 3305-3310

Google Scholar: [Author Only](#) [Title Only](#) [Author and Title](#)

Almagro Armenteros JJ, Sønderby CK, Sønderby SK, Nielsen H, Winther O (2017) DeepLoc: prediction of protein subcellular localization using deep learning. Bioinformatics 33: 3387-3395

Google Scholar: [Author Only](#) [Title Only](#) [Author and Title](#)

Asif MH, Lakhwani D, Pathak S, Gupta P, Bag SK, Nath P, Trivedi PK (2014) Transcriptome analysis of ripe and unripe fruit tissue of banana identifies major metabolic networks involved in fruit ripening process. BMC plant biology 14: 316

Google Scholar: [Author Only](#) [Title Only](#) [Author and Title](#)

Bantan-Polak T, Kassai M, Grant KB (2001) A comparison of fluorescamine and naphthalene-2, 3-dicarboxaldehyde fluorogenic reagents for microplate-based detection of amino acids. Analytical biochemistry 297: 128-136

Google Scholar: [Author Only](#) [Title Only](#) [Author and Title](#)

Bernier F, Berna A (2001) Germins and germin-like proteins: plant do-all proteins. But what do they do exactly? Plant Physiology and Biochemistry 39: 545-554

Google Scholar: [Author Only](#) [Title Only](#) [Author and Title](#)

Bhuiyan F, Campos NA, Swennen R, Carpentier S (2020) Characterizing fruit ripening in plantain and Cavendish bananas: A proteomics approach. Journal of Proteomics 214: 103632

Google Scholar: [Author Only](#) [Title Only](#) [Author and Title](#)

Blainski A, Lopes GC, De Mello JCP (2013) Application and analysis of the folin ciocalteu method for the determination of the total phenolic content from *Limonium brasiliense* L. Molecules 18: 6852-6865

Google Scholar: [Author Only](#) [Title Only](#) [Author and Title](#)

Bradford MM (1976) A rapid and sensitive method for the quantitation of microgram quantities of protein utilizing the principle of protein-dye binding. Analytical biochemistry 72: 248-254

Google Scholar: [Author Only](#) [Title Only](#) [Author and Title](#)

Burg SP (1962) The physiology of ethylene formation. Annual Review of Plant Physiology 13: 265-302

Google Scholar: [Author Only](#) [Title Only](#) [Author and Title](#)

Buts K, Michielssens S, Hertog M, Hayakawa E, Cordewener J, America A, Nicolai B, Carpentier S (2014) Improving the identification rate of data independent label-free quantitative proteomics experiments on non-model crops: A case study on apple fruit. Journal of Proteomics 105: 31-45

Google Scholar: [Author Only](#) [Title Only](#) [Author and Title](#)

Campos NA, Swennen R, Carpentier SC (2018) The Plantain Proteome, a Focus on Allele Specific Proteins Obtained from Plantain Fruits. Proteomics 18: 1700227

Google Scholar: [Author Only](#) [Title Only](#) [Author and Title](#)

Carpentier S, Dens K, Van den houwe I, Swennen R, Panis B (2007) Lyophilization, a Practical Way to Store and Transport Tissues Prior to Protein Extraction for 2DE Analysis? Proteomics 7: 64-69

Google Scholar: [Author Only](#) [Title Only](#) [Author and Title](#)

Carpentier S, Witters E, Laukens K, Deckers P, Swennen R, Panis B (2005) Preparation of protein extracts from recalcitrant plant tissues: An evaluation of different methods for two-dimensional gel electrophoresis analysis. Proteomics 5: 2497-2507

Google Scholar: [Author Only](#) [Title Only](#) [Author and Title](#)

Carreel F, De Leon DG, Lagoda P, Lanaud C, Jenny C, Horry J-P, Du Montcel HT (2002) Ascertaining maternal and paternal lineage within *Musa* by chloroplast and mitochondrial DNARFLP analyses. Genome 45: 679-692

Google Scholar: [Author Only](#) [Title Only](#) [Author and Title](#)

Colombié S, Beauvoit B, Nazaret C, Bénard C, Vercambre G, Le Gall S, Biais B, Cabasson C, Maucourt M, Bernillon S (2017) Respiration climacteric in tomato fruits elucidated by constraint-based modelling. New Phytologist 213: 1726-1739

Google Scholar: [Author Only](#) [Title Only](#) [Author and Title](#)

Colombié S, Nazaret C, Bénard C, Biais B, Mengin V, Solé M, Fouillen L, Dieuaide-Noubhani M, Mazat JP, Beauvoit B (2015) Modelling central metabolic fluxes by constraint-based optimization reveals metabolic reprogramming of developing *Solanum lycopersicum* (tomato) fruit. The Plant Journal 81: 24-39

Google Scholar: [Author Only](#) [Title Only](#) [Author and Title](#)

Cordenunsi-Lysenko BR, Nascimento JRO, Castro-Alves VC, Purgatto E, Fabi JP, Peroni-Okyta FHG (2019) The starch is (not) just another brick in the wall: The primary metabolism of sugars during banana ripening. Frontiers in plant science 10

Google Scholar: [Author Only](#) [Title Only](#) [Author and Title](#)

Cordenunsi BR, Lajolo FM (1995) Starch breakdown during banana ripening: sucrose synthase and sucrose phosphate synthase. Journal of agricultural and food chemistry 43: 347-351

Google Scholar: [Author Only](#) [Title Only](#) [Author and Title](#)

Crouch H, Crouch J, Madsen S, Vuylsteke D, Ortiz R (2000) Comparative analysis of phenotypic and genotypic diversity among plantain landraces (Musa spp., AAB group). Theoretical and Applied Genetics 101: 1056-1065

Google Scholar: [Author Only](#) [Title Only](#) [Author and Title](#)

Da Mota RV, Cordenunsi BR, Do Nascimento JR, Purgatto E, Rosseto MR, Lajolo FM (2002) Activity and expression of banana starch phosphorylases during fruit development and ripening. Planta 216: 325-333

Google Scholar: [Author Only](#) [Title Only](#) [Author and Title](#)

Dadzie B, Orchard J (1997) Routine post-harvest screening of banana/plantain hybrids: criteria and methods. INIBAP Technical Guidelines No. 2. In. INIBAP

Google Scholar: [Author Only](#) [Title Only](#) [Author and Title](#)

do Nascimento JRO, Cordenunsi BR, Lajolo FM (2000) Sucrose synthase activity and expression during development and ripening in bananas. Journal of plant physiology 156: 605-611

Google Scholar: [Author Only](#) [Title Only](#) [Author and Title](#)

Droc G, Lariviere D, Guignon V, Yahiaoui N, This D, Garsmeur O, Dereeper A, Hamelin C, Argout X, Dufayard J-F (2013) The banana genome hub. Database 2013

Google Scholar: [Author Only](#) [Title Only](#) [Author and Title](#)

Du L, Song J, Forney C, Palmer LC, Fillmore S, Zhang Z (2016) Proteome changes in banana fruit peel tissue in response to ethylene and high-temperature treatments. Horticulture research 3: 1-12

Google Scholar: [Author Only](#) [Title Only](#) [Author and Title](#)

El-Sharkawy I, Mila I, Bouzayen M, Jayasankar S (2010) Regulation of two germin-like protein genes during plum fruit development. Journal of experimental botany 61: 1761-1770

Google Scholar: [Author Only](#) [Title Only](#) [Author and Title](#)

Entwistle G, Rees T (1988) Enzymic capacities of amyloplasts from wheat (Triticum aestivum) endosperm. Biochemical Journal 255: 391-396

Google Scholar: [Author Only](#) [Title Only](#) [Author and Title](#)

Farauh M, Rivero RM, Sadka A, Blumwald E (2018) Ethylene regulation of sugar metabolism in climacteric and non-climacteric plums. Postharvest Biology and Technology 139: 20-30

Google Scholar: [Author Only](#) [Title Only](#) [Author and Title](#)

Fils-Lycaon B, Julianus P, Chillet M, Galas C, Hubert O, Rinaldo D, Mbéguié-A-Mbéguié D (2011) Acid invertase as a serious candidate to control the balance sucrose versus (glucose+ fructose) of banana fruit during ripening. Scientia horticulturae 129: 197-206

Google Scholar: [Author Only](#) [Title Only](#) [Author and Title](#)

Gibon Y, Vigeolas H, Tiessen A, Geigenberger P, Stitt M (2002) Sensitive and high throughput metabolite assays for inorganic pyrophosphate, ADPGlc, nucleotide phosphates, and glycolytic intermediates based on a novel enzymic cycling system. The Plant Journal 30: 221-235

Google Scholar: [Author Only](#) [Title Only](#) [Author and Title](#)

Hawkins C, Ginzburg D, Zhao K, Dwyer W, Xue B, Xu A, Rice S, Cole B, Paley S, Karp P (2021) Plant Metabolic Network 15: A resource of genome-wide metabolism databases for 126 plants and algae. Journal of Integrative Plant Biology

Google Scholar: [Author Only](#) [Title Only](#) [Author and Title](#)

Hendriks JH, Kolbe A, Gibon Y, Stitt M, Geigenberger P (2003) ADP-glucose pyrophosphorylase is activated by posttranslational redox-modification in response to light and to sugars in leaves of Arabidopsis and other plant species. Plant physiology 133: 838-849

Google Scholar: [Author Only](#) [Title Only](#) [Author and Title](#)

Hofius D, Börnke FA (2007) Photosynthesis, carbohydrate metabolism and source-sink relations. In Potato biology and biotechnology. Elsevier, pp 257-285

Google Scholar: [Author Only](#) [Title Only](#) [Author and Title](#)

Keller A, Nesvizhskii A, Kolker E, Aebersold R (2002) An explanation of the Peptide Prophet algorithm developed. Anal. Chem 74: 5383-5392

Google Scholar: [Author Only](#) [Title Only](#) [Author and Title](#)

Kuang JF, Wu CJ, Guo YF, Walther D, Shan W, Chen JY, Chen L, Lu WJ (2021) Deciphering transcriptional regulators of banana fruit ripening by regulatory network analysis. Plant biotechnology journal 19: 477-489

Google Scholar: [Author Only](#) [Title Only](#) [Author and Title](#)

Li T, Yun Z, Wu Q, Qu H, Duan X, Jiang Y (2019) Combination of Transcriptomic, Proteomic, and Metabolomic Analysis Reveals the Ripening Mechanism of Banana Pulp. *Biomolecules* 9: 523

Google Scholar: [Author Only](#) [Title Only](#) [Author and Title](#)

Lü P, Yu S, Zhu N, Chen Y-R, Zhou B, Pan Y, Tzeng D, Fabi JP, Argyris J, Garcia-Mas J (2018) Genome encode analyses reveal the basis of convergent evolution of fleshy fruit ripening. *Nature Plants* 4: 784-791

Google Scholar: [Author Only](#) [Title Only](#) [Author and Title](#)

Ma Y, Kanakousaki K, Buttitta L (2015) How the cell cycle impacts chromatin architecture and influences cell fate. *Frontiers in Genetics* 6

Google Scholar: [Author Only](#) [Title Only](#) [Author and Title](#)

Maeshima M (2000) Vacuolar H⁺-pyrophosphatase. *Biochimica et Biophysica Acta (BBA)-Biomembranes* 1465: 37-51

Google Scholar: [Author Only](#) [Title Only](#) [Author and Title](#)

Mainardi JA, Purgatto E, Vieira A, Bastos WA, Cordenunsi BR, Oliveira do Nascimento JR, Lajolo FM (2006) Effects of ethylene and 1-methylcyclopropene (1-MCP) on gene expression and activity profile of α -1, 4-glucan-phosphorylase during banana ripening. *Journal of agricultural and food chemistry* 54: 7294-7299

Google Scholar: [Author Only](#) [Title Only](#) [Author and Title](#)

Martin G, Baurens F-C, Droc G, Rouard M, Cenci A, Kilian A, Hastie A, Doležel J, Aury J-M, Alberti A (2016) Improvement of the banana "Musa acuminata" reference sequence using NGS data and semi-automated bioinformatics methods. *BMC genomics* 17: 243

Google Scholar: [Author Only](#) [Title Only](#) [Author and Title](#)

Mollering H (1985) L-(-) malate. In HU Bergmeyer, ed, *Methods of enzymatic analysis*, Vol 7. VCH Verlagsgesellschaft, Weinheim, Germany, pp 39-47

Google Scholar: [Author Only](#) [Title Only](#) [Author and Title](#)

Nesvizhskii AI, Keller A, Kolker E, Aebersold R (2003) A statistical model for identifying proteins by tandem mass spectrometry. *Analytical chemistry* 75: 4646-4658

Google Scholar: [Author Only](#) [Title Only](#) [Author and Title](#)

Neuhaus H, Ertes M (2000) Nonphotosynthetic metabolism in plastids. *Annual review of plant biology* 51: 111-140

Google Scholar: [Author Only](#) [Title Only](#) [Author and Title](#)

Nguyen-Quoc B, Foyer CH (2001) A role for 'futile cycles' involving invertase and sucrose synthase in sucrose metabolism of tomato fruit. *Journal of Experimental Botany* 52: 881-889

Google Scholar: [Author Only](#) [Title Only](#) [Author and Title](#)

Niittylä T, Messerli G, Trevisan M, Chen J, Smith AM, Zeeman SC (2004) A previously unknown maltose transporter essential for starch degradation in leaves. *Science* 303: 87-89

Google Scholar: [Author Only](#) [Title Only](#) [Author and Title](#)

Orth JD, Thiele I, Palsson BØ (2010) What is flux balance analysis? *Nature biotechnology* 28: 245-248

Google Scholar: [Author Only](#) [Title Only](#) [Author and Title](#)

Osorio S, Nunes-Nesi A, Stratmann M, Fernie A (2013) Pyrophosphate levels strongly influence ascorbate and starch content in tomato fruit. *Frontiers in plant science* 4: 308

Google Scholar: [Author Only](#) [Title Only](#) [Author and Title](#)

Patzke K, Prananingrum P, Klemens PA, Trentmann O, Rodrigues CM, Keller I, Fernie AR, Geigenberger P, Bölder B, Lehmann M (2019) The plastidic sugar transporter pSuT influences flowering and affects cold responses. *Plant physiology* 179: 569-587

Google Scholar: [Author Only](#) [Title Only](#) [Author and Title](#)

Paul V, Pandey R, Srivastava GC (2012) The fading distinctions between classical patterns of ripening in climacteric and non-climacteric fruit and the ubiquity of ethylene-an overview. *Journal of Food Science and Technology* 49: 1-21

Google Scholar: [Author Only](#) [Title Only](#) [Author and Title](#)

Purgatto E, Lajolo FM, do Nascimento JRO, Cordenunsi BR (2001) Inhibition of β -amylase activity, starch degradation and sucrose formation by indole-3-acetic acid during banana ripening. *Planta* 212: 823-828

Google Scholar: [Author Only](#) [Title Only](#) [Author and Title](#)

Ram HM, Ram M, Steward F (1962) Growth and development of the banana plant: 3. A. The origin of the inflorescence and the development of the flowers: B. The structure and development of the fruit. *Annals of Botany* 26: 657-673

Google Scholar: [Author Only](#) [Title Only](#) [Author and Title](#)

Rohart F, Gautier B, Singh A, Lê Cao K-A (2017) mixOmics: An R package for 'omics feature selection and multiple data integration. *PLoS computational biology* 13: e1005752

Google Scholar: [Author Only](#) [Title Only](#) [Author and Title](#)

Searle BC (2010) Scaffold: a bioinformatic tool for validating MS/MS-based proteomic studies. *Proteomics* 10: 1265-1269

Google Scholar: [Author Only](#) [Title Only](#) [Author and Title](#)

Shiga TM, Soares CA, Nascimento JR, Purgatto E, Lajolo FM, Cordenunsi BR (2011) Ripening-associated changes in the amounts of starch and non-starch polysaccharides and their contributions to fruit softening in three banana cultivars. *Journal of the Science of Food and Agriculture* 91: 1511-1516

Google Scholar: [Author Only](#) [Title Only](#) [Author and Title](#)

Simmonds NW (1953) The development of the banana fruit. *Journal of Experimental Botany* 4: 87-105

Google Scholar: [Author Only](#) [Title Only](#) [Author and Title](#)

Simmonds NW (1962) The evolution of the bananas. Longmans, Green., London

Google Scholar: [Author Only](#) [Title Only](#) [Author and Title](#)

Singh A, Shannon CP, Gautier B, Rohart F, Vacher M, Tebbutt SJ, Lê Cao K-A (2019) DIABLO: an integrative approach for identifying key molecular drivers from multi-omics assays. *Bioinformatics* 35: 3055-3062

Google Scholar: [Author Only](#) [Title Only](#) [Author and Title](#)

Smith JJ, Ververidis P, John P (1992) Characterization of the ethylene-forming enzyme partially purified from melon. *Phytochemistry* 31: 1485-1494

Google Scholar: [Author Only](#) [Title Only](#) [Author and Title](#)

Soares CA, Peroni-Okita FHGa, Cardoso MB, Shitakubo R, Lajolo FM, Cordenunsi BR (2011) Plantain and banana starches: granule structural characteristics explain the differences in their starch degradation patterns. *Journal of Agricultural and Food Chemistry* 59: 6672-6681

Google Scholar: [Author Only](#) [Title Only](#) [Author and Title](#)

Soubeyrand E, Colombié S, Beauvoit B, Dai Z, Cluzet S, Hilbert G, Renaud C, Maneta-Peyret L, Dieuaide-Noubhani M, Mérillon J-M (2018) Constraint-based modeling highlights cell energy, redox status and α -ketoglutarate availability as metabolic drivers for anthocyanin accumulation in grape cells under nitrogen limitation. *Frontiers in plant science* 9: 421

Google Scholar: [Author Only](#) [Title Only](#) [Author and Title](#)

Stitt M, Lilley RM, Gerhardt R, Heldt HW (1989) Metabolite levels in specific cells and subcellular compartments of plant leaves. *Methods in enzymology* 174: 518-552

Google Scholar: [Author Only](#) [Title Only](#) [Author and Title](#)

Streb S, Zeeman SC (2012) Starch metabolism in Arabidopsis. *The Arabidopsis book/American Society of Plant Biologists* 10

Google Scholar: [Author Only](#) [Title Only](#) [Author and Title](#)

Tetlow IJ, Morell MK, Emes MJ (2004) Recent developments in understanding the regulation of starch metabolism in higher plants. *Journal of experimental botany* 55: 2131-2145

Google Scholar: [Author Only](#) [Title Only](#) [Author and Title](#)

Tobias RB, Boyer CD, Shannon JC (1992) Alterations in carbohydrate intermediates in the endosperm of starch-deficient maize (*Zea mays* L.) genotypes. *Plant Physiology* 99: 146-152

Google Scholar: [Author Only](#) [Title Only](#) [Author and Title](#)

Toledo TT, Nogueira SB, Cordenunsi BR, Gozzo FC, Pilau EJ, Lajolo FM, do Nascimento JRO (2012) Proteomic analysis of banana fruit reveals proteins that are differentially accumulated during ripening. *Postharvest Biology and Technology* 70: 51-58

Google Scholar: [Author Only](#) [Title Only](#) [Author and Title](#)

van Wesemael J, Hueber Y, Kissel E, Campos N, Swennen R, Carpentier S (2018) Homeolog expression analysis in an allotriploid non-model crop via integration of transcriptomics and proteomics. *Scientific reports* 8: 1353

Google Scholar: [Author Only](#) [Title Only](#) [Author and Title](#)

Vuylsteke D, Ortiz R, Pasberg-Gauhl C, Gauhl F, Gold C, Ferris S, Speijer P (1993) Plantain and banana research at the International Institute of Tropical Agriculture. *HortScience* 28: 874-971

Google Scholar: [Author Only](#) [Title Only](#) [Author and Title](#)

Wang Z, Miao H, Liu J, Xu B, Yao X, Xu C, Zhao S, Fang X, Jia C, Wang J, Zhang J, Li J, Xu Y, Wang J, Ma W, Wu Z, Yu L, Yang Y, Liu C, Guo Y, Sun S, Baurens F-C, Martin G, Salmon F, Garsmeur O, Yahiaoui N, Hervouet C, Rouard M, Laboureau N, Habas R, Ricci S, Peng M, Guo A, Xie J, Li Y, Ding Z, Yan Y, Tie W, D'Hont A, Hu W, Jin Z (2019) Musa balbisiana genome reveals subgenome evolution and functional divergence. *Nature Plants* 5: 810-821

Google Scholar: [Author Only](#) [Title Only](#) [Author and Title](#)

Weber A, Servaites JC, Geiger DR, Kofler H, Hille D, Gröner F, Hebbeker U, Flügge U-I (2000) Identification, purification, and molecular cloning of a putative plastidic glucose translocator. *The Plant Cell* 12: 787-801

Google Scholar: [Author Only](#) [Title Only](#) [Author and Title](#)

White PJ (2002) Recent advances in fruit development and ripening: an overview. *Journal of Experimental Botany* 53: 1995-2000

Google Scholar: [Author Only](#) [Title Only](#) [Author and Title](#)

Xiao Yy, Kuang Jf, Qi Xn, Ye Yj, Wu ZX, Chen Jy, Lu Wj (2018) A comprehensive investigation of starch degradation process and identification of a transcriptional activator Mab HLH 6 during banana fruit ripening. Plant biotechnology journal 16: 151-164

Google Scholar: [Author Only](#) [Title Only](#) [Author and Title](#)

Zhang T, Li W, Xie R, Xu L, Zhou Y, Li H, Yuan C, Zheng X, Xiao L, Liu K (2020) CpARF2 and CpEIL1 interact to mediate auxin–ethylene interaction and regulate fruit ripening in papaya. The Plant Journal 103: 1318-1337

Google Scholar: [Author Only](#) [Title Only](#) [Author and Title](#)

Zhao Z, Zhang Y, Liu X, Zhang X, Liu S, Yu X, Ren Y, Zheng X, Zhou K, Jiang L (2013) A role for a dioxygenase in auxin metabolism and reproductive development in rice. Developmental Cell 27: 113-122

Google Scholar: [Author Only](#) [Title Only](#) [Author and Title](#)